Effectiveness and Energy Saving Potential of Biofiltration of Indoor Air in U.S. Offices

A thesis submitted to the Faculty of

Drexel University

by

Bryan E. Cummings

in partial fulfillment of the requirements for the degree of

Master of Science in Architectural Engineering

June 2017

TABLE OF CONTENTS

LIST OF TABLES

LIST OF FIGURES

ABSTRACT

Ventilation accounts for about 8-10% of energy consumed by commercial buildings in the U.S. Alternative strategies are being developed which can clean indoor air while simultaneously saving energy on ventilation. This work investigates biowalls as a ventilation alternative, and conducts Monte Carlo simulations to determine its effectiveness within the U.S. office stock as a means of cleaning the indoor air of VOCs and as a measure to save energy on ventilation. Savings were determined by comparing the ventilation energy required to maintain the same VOC concentrations for two indoor atmospheric box models: one incorporating a biowall and the other without. A sensitivity analysis was also conducted to determine the most influential parameters, and for a user to predict savings based upon known building parameters. It was found that the largest criterion for energy savings is climate. Median annual ventilation savings ranged from about 1 $/m^2 in temperate locations such as San Francisco, to about 4 $/m^2 in more extreme climates such as those found in Miami or Alaska. The median annual amount of energy saved on cooling in Miami was about 35 kWh/m^2, about three times less than the 110 kWh/m^2 of heating energy saved in Alaska; this difference caused by the nature of electric cooling versus gas-fired heating. This discrepancy is equilibrated when accounting for the cost of the respective utilities. While operating a biowall resulted in a net decrease in energy consumption in the majority of cases, operating cost increased significantly due to the projected cost of plant upkeep, which, with a median of about $3800/year, accounted for over half of the total biowall operational cost. Total biowall operating cost was not impacted by climate. It was instead highly variable but can be controlled by the design of the biowall itself and it building it occupies.

NOMENCLATURE

Abbreviations

IAQ	indoor air quality
SBS	sick building syndrome
AHU	air handling unit
VOC	volatile organic compound
VVOC	very volatile organic compound
TVOC	total volatile organic compounds
DD	degree-days
DH	degree-hours
N	normal distribution
LN	lognormal distribution
U	uniform distribution
GM	geometric mean
GSD	geometric standard deviation
SD	standard deviation
TMY	typical meteorological year
IECC	international energy conservation code

Subscripts

b	biowall
f	floor
r	recirculation
v	ventilation
1	scenario 1
2	scenario 2
bal	balance point
set	setpoint
h	heating
c	cooling
w	water
e	electricity
g	gas

Variables

V	volume
A	area
H_c	ceiling height
R	relative biowall size
C	concentration
E	energy, if subscripted emissions, if not subscripted
λ	air exchange rate
Q	flow rate
V	flux
CADR	clean air delivery rate
T	temperature
RH	relative humidity
W	humidity ratio
HDH	heating degree-hours
CDH	cooling degree-hours
LEH	latent enthalpy hours
η	efficiency
COP	coefficient of performance
h_L	hours of lighting
LPD	lighting power density
PPD	pump power density
FPD	fan power density
P	Price
M	maintenance cost
S	cost or savings
pRed	percent reduced
Γ	Effectiveness
c	linear regression coefficient
β	standardized regression coefficient

1. INTRODUCTION

Indoor air quality (IAQ) can have a considerable impact on our lives, since citizens of developed countries spend approximately 90% of their time indoors (e.g., Klepeis et al., 2001). The U.S. Environmental Protection Agency (EPA) characterizes indoor air as being significantly more polluted than outdoor air (US EPA, 2017a). This condition is caused by both an abundance of indoor pollutant sources and the accumulation of pollutants within the building's envelope. It has been suggested that between 65,000 and 150,000 deaths per year in the U.S. are caused by indoor air pollution (Lomborj, 2002). Buildings with good IAQ provide occupants with fewer instances of sick building syndrome (SBS), increased comfort and productivity, and a reduced risk of long-term health effects. Three general strategies for improving IAQ are the removal of pollutant sources, ventilation, and using air cleaners to purify indoor air (US EPA, 2017b).

The most common method of improving IAQ is ventilation (Wargocki et al., 2002), which is the process of diluting stale or more polluted indoor air with presumably clean outdoor air, using airflow generated either mechanically or by means of natural convection. In the United States, the outdoor air is generally considered clean enough for ventilation purposes if the region is in attainment with the National Ambient Air Quality Standards (AHSRAE 62.1, 2010). Furthermore, studies have shown that ventilation rates below 25 L/s per person correlate with SBS symptoms (Sundell et al., 2010), which are significantly aggravated when ventilation falls below 10 L/s per person (Wargocki et al., 2002).

Ventilation inherently uses energy and costs money because outdoor air must be treated to have thermally comfortable indoor conditions. Commercial buildings consume about 20% of primary energy in the U.S. (US DOE, 2012). Heating, ventilation, and air conditioning (HVAC) accounts for 30 to 40% of U.S. commercial buildings' energy consumption (US DOE, 2012; US EIA, 2017), about 25% of which is due to ventilation (US EIA, 2017; Fisk et al., 2012). The benefits of ventilation on occupant health are well known and are cost effective despite the resulting increase in energy consumption (e.g., Fisk, 2000). However, ever increasing energy consumption

while striving to achieve higher IAQ is not the most sustainable practice. This case is strengthened because most of our energy is derived from fossil fuels (US EIA, 2016a), but it also has validity regardless of the energy source. As the green building movement continues, improving IAQ while simultaneously reducing energy consumption is increasingly demanded (e.g., USGBC). Therefore, other strategies of improving IAQ must also be explored.

Regarding source removal, in order to remove pollutant sources, the source must be known and the removal must be technically and economically feasible, which is rarely the case (Guieysse et al., 2008). Also, there may be hundreds or more of volatile organic compounds (VOC) in buildings, making total source control of all of the VOCs impossible. Therefore, besides ventilation, purification of indoor air using air cleaners is the best option for improving IAQ that may also allow for energy-saving reductions in mechanical ventilation. This work explores the feasibility of using biofiltration to purify and remove VOCs from indoor air.

While IAQ is dependent on a wide variety of airborne constituents, including particulate matter, biological agents, radon, and gases such as CO, CO_2, NO_X, and VOCs (Guieysse et al., 2008), the VOC component particularly may be a primary cause of many SBS symptoms and other health problems associated with indoor air (Wallace, 2001; Jones, 1999; Wieslander et al., 1997; Yu and Crump, 1998). VOCs are generally defined as organic compounds with high enough vapor pressures that they readily evaporate under normal indoor atmospheric conditions of temperature and pressure. At any given time, hundreds of VOCs are in indoor air at widely varying concentrations. VOCs are continually released into the indoor environment from a variety of sources, including furnishings, building materials, office equipment, and household products (US EPA, 2017c). Even originally harmless VOCs can react with ozone (O_3) or the hydroxyl radical (OH) to produce secondary organic aerosols and oxygenated gas-phase contaminants (Waring, 2014), which can then be responsible for harmful impacts.

Sidheswaren et al. (2011) suggests that an air cleaner, in their case an activated carbon filter, which removes VOCs from the supply airstream with a 15 to 20% efficiency at a face velocity through the filter of about 0.52 m/s, allows for an approximately 50% reduction in ventilation. While there are currently well-established and efficient air purification technologies that are effective at removing particulate matter, similar technologies for removing VOCs are far less developed (Guieysse et al., 2008), which perhaps further explains the current prevalence of relying on ventilation to improve IAQ regarding VOCs. Activated carbon filters are effective for many organic gases, but have not been shown to remove well very volatile organic compounds (VVOC), such as formaldehyde (Sidheswaren et al., 2011). For removal of VVOCs and VOCs, botanical purification has been suggested to be an effective technology (Chen et al., 2005).

Broadly speaking, biofiltration refers to any biological process that removes contaminants from an air or water stream. Chamber studies have shown that potted plants can reduce the ambient concentration of VOCs in the chamber (e.g., Wolverton et al., 1989), known as botanical purification. The root and soil system is responsible for the most VOC removal, and large commercial botanical purifiers for treating indoor air now exist in the form of a plant-assisted botanical biotrickling filter (Darlington et al., 2000; Darlington et al., 2001), a.k.a. a “biowall”.

In essence, the biowall is a vertical aeroponic garden, diagrammed in Figure 1 and annotated as follows. Plants (a) with exposed roots occupy an artificial rooting medium (b) that is kept moist by a constant trickling supply of water (c), pumped (d) from a catch basin (e) beneath the wall. Fans (f) pull air from the occupied space, through the rooting media, and toward the building’s air handling unit (AHU) to be conditioned and redistributed throughout the building. VOCs are removed from the air stream as it passes through the plant and root substrate.

Biofiltration generally occurs through a two-step process, being the transfer of pollutants from the airstream followed by biodegradation (Malhautier ae al., 2005). Pollutants partition either into an aqueous solution or directly onto the plant or root media. For aqueous partitioning, the Henry’s constant of a VOC governs its concentration in the aqueous solution, as proportional

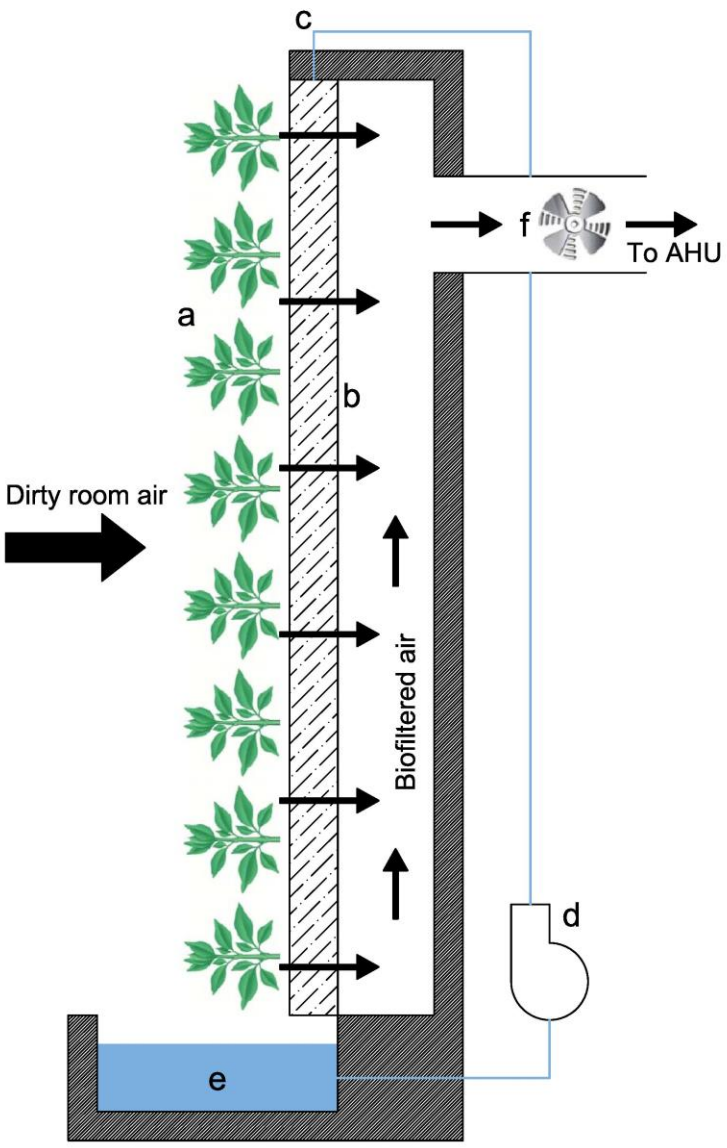

Figure 1 Illustration of a biowall, its components, and flows, where: a. aeroponic plants; b. porous rooting medium; c. trickling water supply; d. water recirculating pump; e. water within catch-basin; and f. fan distributing biofiltered air to an AHU.

to its air concentration. Otherwise, pollutants will adsorb directly onto the root media or plant structure. Soreanu et al. (2013) reviews five independent biodegradation mechanisms capable by botanical purifiers: (1) biodegradation in the rhizosphere by microorganism; (2) phytoextraction, the removal of pollutants from the liquid phase; (3) stomatal uptake, removal of pollutants from the gas phase by plant leaves; (4) phytodegredation by enzymatic catalysis inside plant tissues;

and (5) phytovolatilization. However, it is suggested that the preferred route of biodegradation occurs by rhizosphere microbial activity. Further research is required to gain full insight into the exact removal mechanisms of specific VOCs by specific plant-air systems.

Because of the continual biological consumption of pollutants, their concentrations in the soil, root media, and aqueous solution always remain low, resulting in a continuous driving force of removal from the airstream (Malhautier et al., 2005). This continuous removal gives biological filtration an advantage compared with conventional physio-chemical means of gaseous pollutant removal, such as adsorption, where the transfer of pollutants from the airstream slows with time as the adsorbent saturates. Conventional adsorbents also risk desorption of pollutants back into the air stream based on other factors such as concentration and temperature. Adsorbents also must be periodically desorbed, emitting pollutants into the surrounding environment or other means of storage and requiring energy for the process. Biological filtration, on the other hand, alleviates this problem, as the harmful pollutants are converted to harmless—potentially useful—products, including biomass, metabolic end-products, or carbon dioxide and water.

Though biowalls have some advantages with their VOC removal methods, they are not self-sustaining systems and require energy and effort to remain operational and well-functioning. For instance, vegetation suitable for biowalls are typically native to tropical regions, so supplementary high-intensity lights may be needed to compensate for lack of direct light indoors in some buildings, or also for shorter amounts of daylight in certain geographical regions. Power is required for fans to force air through the root media of the biowall, and for pumps recirculating water to maintain the trickling flow around the plant roots. When the forced air passes over the trickling flow, water evaporates from the root media and reservoir, creating the demand for water to be continuously resupplied to the recirculation loop. Typical biowalls will also require regular plant upkeep. These demands all require the input of energy and/or cost money, so the practical efficacy of a biowall will depend on whether its energy saved by conditioning less ventilation air

outweighs its own energy demands and operating costs. This work uses literature and simulations to explore the performance of biowalls and their cost-effectiveness as compared to ventilation.

2. METHODOLOGY

The methodology consists of two major segments. The first segment describes the procedure to characterize the biowall based on certain biowall and building design parameters. Because biowalls are an emerging technology, good empirical data describing their performance in real buildings does not yet exist. As such, literature on laboratory and room scale biowall VOC removal and typical HVAC system capacities were used to deduce realistic values for relevant parameters. The second segment uses parameters gleaned from the first segment, along with other relevant building and climate inputs, to model the impact of a biowall in a typical office building, from two perspectives. The first is as an IAQ air purifier, considered from a VOC perspective only since they are the target contaminants for removal. The second is as an air purification technology used to reduce ventilation. For this, considering their purification potentials, we determined the cost of operating and maintaining the biowall and then compared it to the cost of energy saved by using a biowall to reduce ventilation by an amount that would maintain an equal VOC concentration to the original ventilation rate.

All parameters were modeled as probability distributions, and simulations were run repeatedly within Monte Carlo operations to capture the diversity among buildings and climate types, and to quantify levels of certainty. Statistical sensitivity analysis of the simulation results for the second segment was performed to reveal those parameters that were the most influential on the outcomes. All simulations were run using MATLAB version R2015b.

2.1. Determining Parameters Relating to Biowalls

Since biowalls are relatively new as a technology, there are no statistical data and few past precedents that describe their performance and design parameters. Therefore, before any

simulation was run, this work first reviewed the literature to compile a good understanding of the parameters relevant to biowalls and their associated assumptions. Largely speaking, the main parameters of interest that needed to be quantified were how well a biowall removes VOCs from the air, the volumetric airflow through the biowall, and the biowall's physical size.

*2.1.1. VOC r*emoval *e*fficiency

Darlington et al. (2001) measured removal efficiencies of toluene, ethylbenzene, and xylene for a laboratory-scale biowall, similar in concept to that in Figure 1. Among other data, Darlington et al. (2001) reported ratios of effluent to influent concentrations of each VOC passing through the biowall, with an experimental matrix that varied both the air flux and temperature of the water wetting the plants. Flux can be related to airflow through the biowall with Equation 1:

$$Q_{\mathrm{b}} = 3600 \cdot v_{\mathrm{b}} A_{\mathrm{b}} \tag{1}$$

where v_{b} (m/s) is the flux of air through the biowall; Q_{b} (m^3/h) is the volumetric flow rate of air through the biowall; A_{b} (m^2) is the area of the biowall; and 3600 is a unit conversion factor. The term v_{b} is written as a velocity with units of m/s, but it can also be represented using the units of m^3/s of air per unit biowall area, as in $m^3/s/m^2$, as a volumetric flux term.

The ratios reported by Darlington et al. (2001) were subtracted from 1 to yield their biowall VOC removal efficiencies, and Figure 2 illustrates a scatter plot of removal efficiency versus flux. Please note that the data used to generate this figure was visually determined using plots in the Darlington et al. (2001) work, and the impact of this error was treated as negligible, since a large standard deviation (SD) was assigned to the removal efficiency in the Monte Carlo operation. Varying neither temperature nor type of VOC created any noticeable trends in removal efficiency in the Darlington et al. (2001) work, so we decided to use all their data to consider stochastically a generic VOC in this analysis, modeled as a function of flux only.

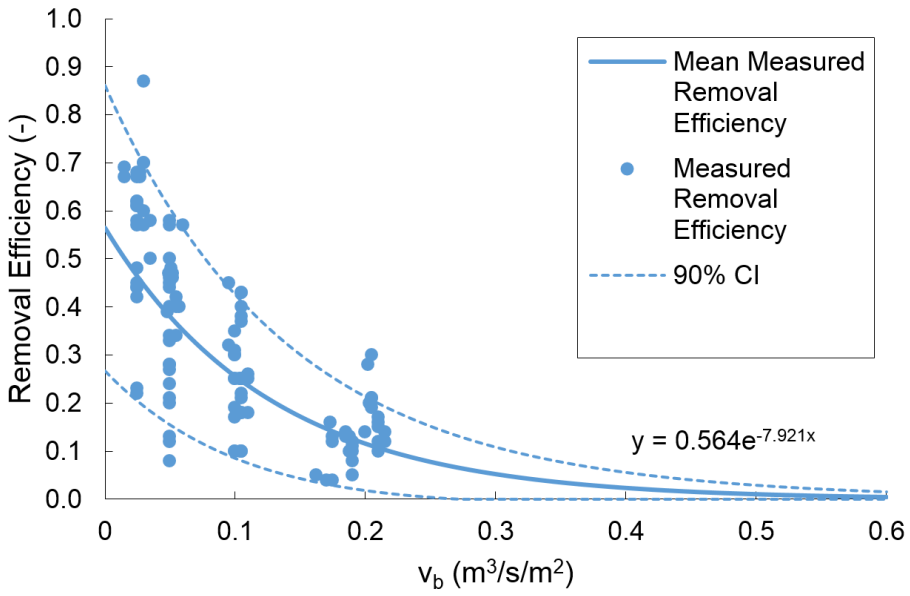

Figure 2 Removal efficiency of toluene, ethylbenzene, and xylene versus flux for biowalls from Darlington et al. (2001).

Both the mean and variance of the biowall removal efficiency decrease with increasing flux. An exponential curve was fit to the removal efficiencies in Figure 2, to be used in the Monte Carlo simulation to define the mean of the removal efficiency distribution at any flux. To define a function for the SD which decreases with flux, the dataset was split into three "bins": low ($0.0 < v_b \leq 0.075$ $m^3/s/m^2$), medium ($0.075 < v_b \leq 0.15$ $m^3/s/m^2$), and high ($v_b > 0.15$ $m^3/s/m^2$) flux. For each bin, a normal distribution, with a mean forced at zero, was fit to the residuals of the removal efficiency data points from the best-fit curve (Figure 3). The calculated SDs for these three distributions were plotted against their data's mean flux in Figure 4. Although these three data points are better fit linearly, an exponentially decaying curve was used instead because it is positive-definite, and SDs cannot be negative. This curve was used in the Monte Carlo simulation to define the SD of the removal efficiency distribution at any flux.

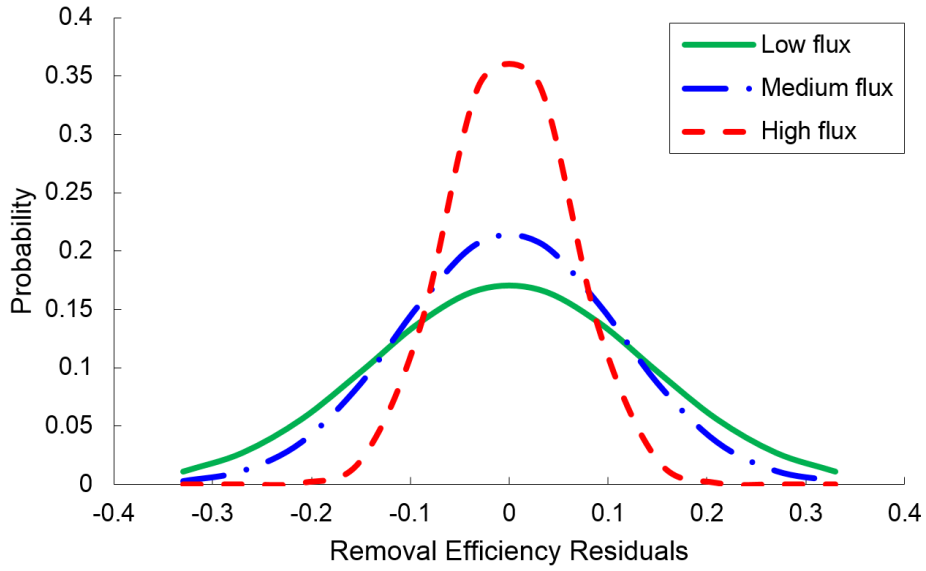

Figure 3 Probability density functions for removal efficiency residuals across each flux bin.

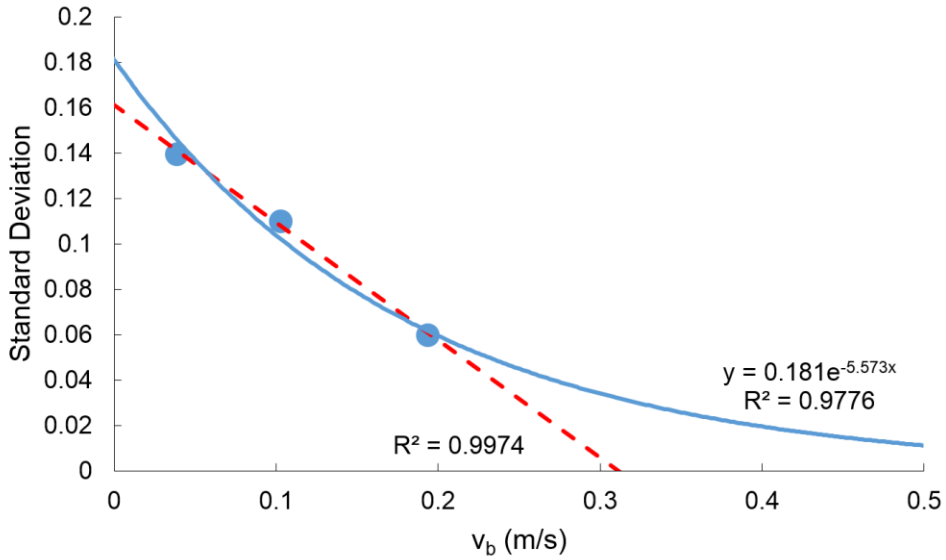

Figure 4 Calculated removal efficiency SD versus average flux for each bin. The best linear (dotted red) and exponential (solid blue) fits are also shown.

2.1.2. Clean air delivery rate

For any indoor air cleaner, its ability to remove a pollutant can be characterized with the clean air delivery rate (CADR), which is the effective volumetric flow rate of clean air that it

provides. It is defined as the product of the flow rate of air through the cleaner and its removal efficiency. For this analysis, this product was considered to be the total CADR (m^3/h):

$$\mathrm{CADR} = Q_\mathrm{b}\eta_\mathrm{b} \tag{2}$$

where η_b is the removal efficiency. Because Q_b, and therefore CADR, is dependent on the size of the biowall (see Equation 1), we considered a normalized CADR for the biowall. $\mathrm{CADR_n}$ (units of $m^3/h/m^2$ or m/h) can be represented by dividing Equation 2 by the biowall area, A_b (m^2):

$$\mathrm{CADR_n} = \frac{Q_\mathrm{b}\eta_\mathrm{b}}{A_\mathrm{b}} \tag{3}$$

Because values for neither Q_b nor A_b are known at this stage, substituting Q_b with the expression from Equation 1 yields:

$$\mathrm{CADR_n} = 3600 \cdot v_\mathrm{b}\eta_\mathrm{b} \tag{4}$$

The removal efficiency data presented in Figure 2 can be manipulated based on this equation to present the relationship between $\mathrm{CADR_n}$ with flux, shown in Figure 5.

Simply put, a larger CADR means that the air cleaner is more effective at removing contaminants. For a biowall, increasing the CADR can be accomplished by either maximizing the $\mathrm{CADR_n}$ or by increasing the size of the biowall. Figure 5 shows that maximum $\mathrm{CADR_n}$ occurs at a flux of ~0.125 m/s. And while biowall size does not have a theoretical maximum value, it does have a practical maximum value. Therefore, this work assumed that the limiting factor of the biowall size was the capacity of the building's HVAC system.

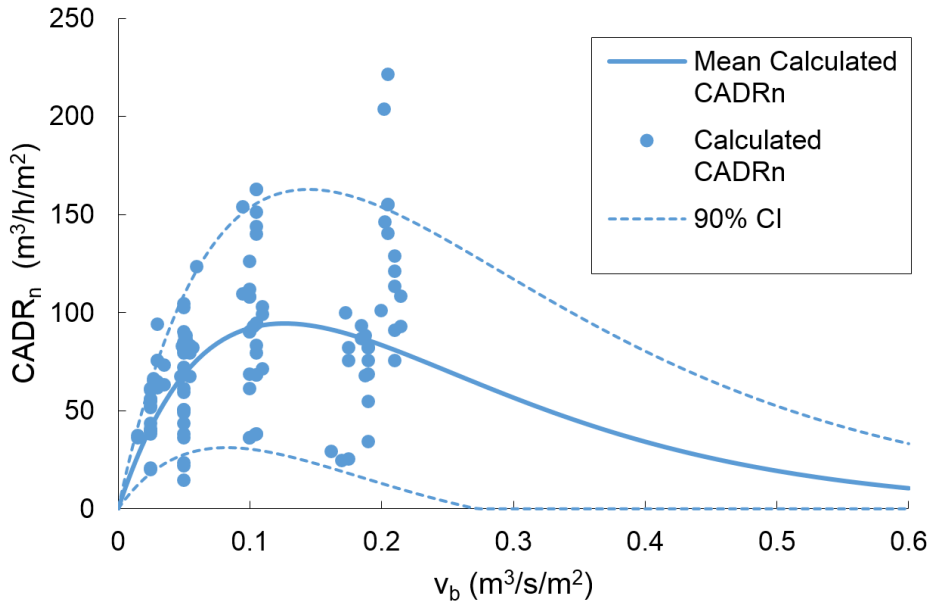

Figure 5 $CADR_n$ versus flux for biowalls. Calculations based on the data in Figure 2 and Equation 4.

2.1.3. Relative biowall size

The biowall was modeled as being integrated into the building's central HVAC system, since this is typically how real examples of biowalls are designed. According to Figure 6, the air

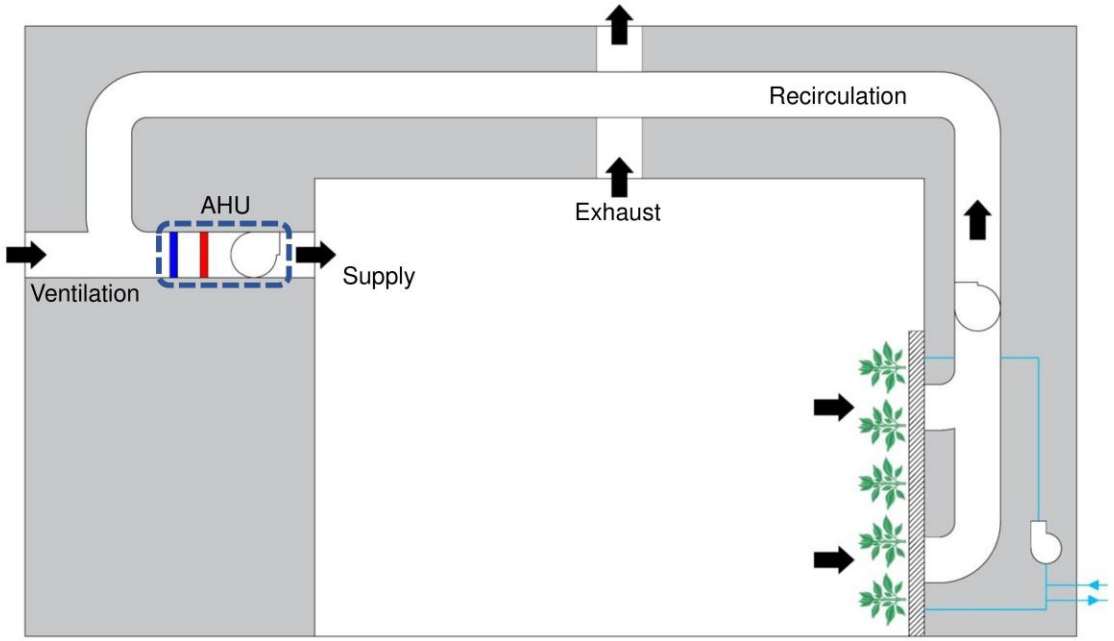

Figure 6 Schematic of integration of biowall within the HVAC system as modeled in this work. Air filtered through the biowall is recirculated, and 100% of recirculated air is biofiltered. Recirculated air meets with ventilated air which are then conditioned by the AHU. Additional air is also exhausted.

pulled through the biowall is sent back to the main air handling unit (AHU) before being resupplied to the occupied spaces. We therefore assumed that the biowall cannot accommodate more flow than the capacity of the recirculation airflow measured in a distribution of real offices (actual parameters described more below). Supply air was not used so that some amount of the HVAC airflow could always be reserved for providing adequate ventilation air if desired.

The recirculation airflow, Q_r (m^3/h), can be expressed as in Equation 5:

$$Q_r = \lambda_r V \tag{5}$$

where λ_r (h^{-1}) is the recirculation air exchange rate; and V (m^3) is the volume of the building. This expression can be normalized by the footprint of the building by dividing through by the floor area of the space served by the HVAC system, A_f (m^2):

$$Q"_r = \frac{\lambda_r V}{A_f} \tag{6}$$

where $Q"_r$ can either be expressed in units of m/h or $m^3/h/m^2$ floor area. Because V is the product of the building's ceiling height, H_c (m), and floor area, Equation 6 can be simplified to:

$$Q"_r = \lambda_r H_c \tag{7}$$

The ratio of $Q"_r$ to flux, after substituting appropriately for the definition of $Q"_r$ represented in Equation 6 and the expression for v_b provided by Equation 1, can be alternatively expressed by:

$$\frac{Q"_{\mathrm{r}}}{v_{\mathrm{b}}} = \frac{\left(\frac{Q_{\mathrm{r}}}{A_{\mathrm{f}}}\right)}{\left(\frac{Q_{\mathrm{b}}}{A_{\mathrm{b}} \cdot 3600}\right)} \tag{8}$$

Because it was assumed that the limiting factor in biowall size is the building's recirculation airflow, Q_b can be set equal to Q_r for the condition of maximizing the biowall's CADR. This, along with using Equation 7 to substitute for $Q"_r$, simplifies to:

$$\frac{\lambda_{\mathrm{r}} H_{\mathrm{c}}}{3600 \cdot v_{\mathrm{b}}} = \frac{A_{\mathrm{b}}}{A_{\mathrm{f}}} \equiv R \tag{9}$$

Here, we define R (m^2/m^2), which is a parameter of the ratio of the area of the biowall to the floor area, hereon referred to as the relative biowall size, presented in form such that neither of the areas need to be known to determine it, under the assumption that the biowall is constructed to maximize CADR (i.e., so that Q_b equals Q_r). In this case, R can be expressed in terms of the flux, as well as the recirculation air exchange rate and ceiling height, both of which have well-known distributions for offices.

2.1.4. Defining v_b and R distributions

A statistical distribution for the parameter R was used in the Monte Carlo operation, along with one for floor area, to set the biowall area for calculations. The R distribution was developed using published distributions of relevant office building parameters in Equation 9. Statistical lognormal distribution metrics were first culled, including those describing ventilation air exchange rates, λ_v (h^{-1}) and H_c for offices, determined by Rackes and Waring (2015), and those describing the primary air exchange rate, λ_p (h^{-1}), determined by Rackes and Waring (2013). Then, an initial Monte Carlo operation was conducted to obtain lognormal distributions for λ_r (where $\lambda_r = \lambda_p - \lambda_v$) and subsequently $Q"_r$ via Equation 7.

The geometric mean (GM) for v_b was set to be 0.125 m/s, under the assumption that the biowall will be operated to maximize the CADR (discussed in section 2.1.2), and the GM for Q''_r from the initial Monte Carlo was determined to be 11.69 m/h. The GM for R was then calculated via Equation 9, which yielded 0.026. The geometric standard deviation (GSD) for both R and v_b was set equal to the GSD calculated for Q''_r of 2.27. This assumption is justified because both parameters must vary together with Q''_r in order to yield a Q_b which equals Q_r. Our calculated result for the GM of R is on the same order as the recommendation by the company Nedlaw Living Walls (2017), who manufactures biowalls, of 1 m^2 of biowall for every 100 m^2 of floor area (R = 0.01).

The sloped lines in the log-log plot presented in Figure 7 shows combinations of R and v_b such that $Q_b = Q_r$, for the median Q_r and 99% confidence interval in U.S. offices, which is the

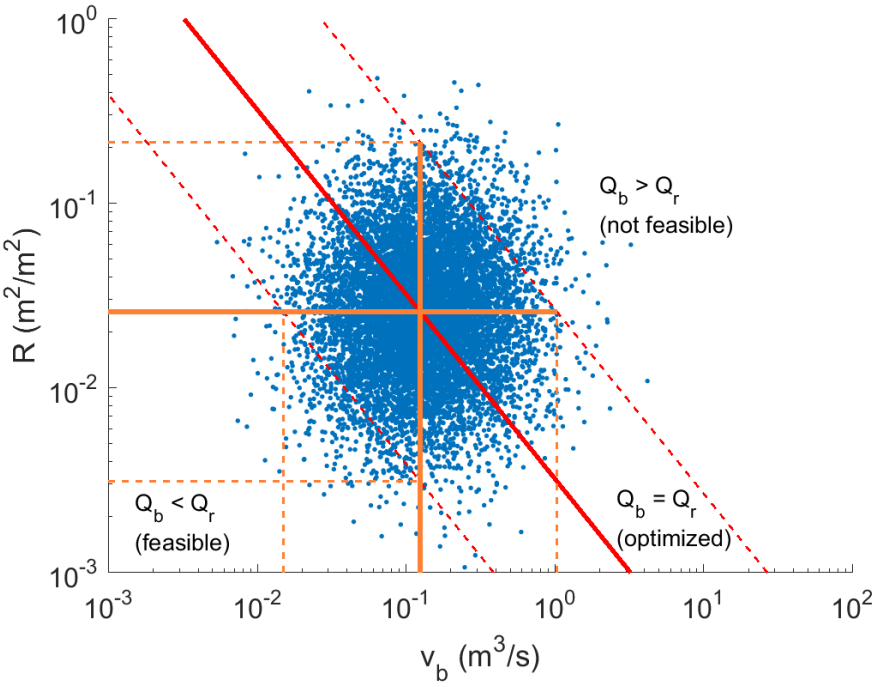

Figure 7 Scattered R and v_b combinations used in the Monte Carlo simulation shown in blue. The red lines represent all combinations where $Q_b = Q_r$, above which $Q_b > Q_r$, which is not feasible, and below which $Q_b < Q_r$, which is not optimized, based on our assumptions. The orange lines represent distribution parameters for R and v_b. Solid lines represent median values, dashed lines denote the 99% confidence intervals.

optimized case where CADR is maximized. Combinations below this line are also feasible, but Q_b is less than Q_r in these cases, so the CADR has room to increase. Combinations above the line are cases where Q_b would be greater than Q_r, exceeding the capacity of the building's HVAC system, therefore considered not feasible. Also shown in the figure are a sample of data points based on the R and v_b distributions determined previously, to be used in the Monte Carlo operation in the following section, which is the optimized case. The figure also shows the GMs and 99% confidence intervals of both R and v_b distributions.

2.2. Energy Simulation

2.2.1. Ventilation reduction

Total volatile organic compound (TVOC) concentrations were considered under steady state conditions in a single-zoned indoor environment containing well-mixed air. Two different scenarios were modeled:

- Scenario 1 being a baseline condition considering air exchange with the outdoors and indoor TVOC emissions, without a biowall, and
- Scenario 2 being a condition that encompasses the assumptions of baseline condition with the addition of a biowall acting as an air cleaner.

The equation used for TVOC concentrations under Scenario 1 is:

$$C_1 = \frac{\lambda_{v,1} C_{out} + \left(E/V\right)}{\lambda_{v,1}} \tag{10}$$

where C_1 (μg/m^3) is the steady state indoor TVOC concentration in Scenario 1; C_{out} (μg/m^3) is the ambient outdoor TVOC concentration; $\lambda_{v,1}$ (h^{-1}) is the baseline ventilation air exchange rate in Scenario 1; and E/V (μg/h·m^3) is the volume normalized emission rate of indoor TVOC. For Scenario 2, the equation for the steady state indoor TVOC concentration becomes:

$$C_2 = \frac{\lambda_{v,2} C_{out} + \left(E/V\right)}{\lambda_{v,2} + \left(\mathrm{CADR}/V\right)} \tag{11}$$

where C_2 (μg/m^3) is the steady state indoor TVOC concentration in Scenario 2; and $\lambda_{v,2}$ (h^{-1}) is the ventilation air exchange rate in Scenario 2.

Because ASHRAE 62.1 specifies minimum ventilation requirements rather than a cap on indoor TVOC concentrations, C_1 was permitted to vary throughout the instantiations (the individual instances or runs of the Monte Carlo simulation) of the Monte Carlo simulation. Therefore, we did not specify a target TVOC concentration to be achieved by using the biowall. Instead, we required that the C_2 be equal to C_1 for each case, which is achieved by operating the building at a lower ventilation rate in Scenario 2 than Scenario 1. The $\lambda_{v,2}$ can then be found by setting Equations 10 and 11 equal to one another and rearranging as follows:

$$\lambda_{v,2} = \lambda_{v,1} - \frac{\lambda_{v,1} C_{out} \mathrm{CADR}}{\left(E/V\right) \cdot V} - \frac{\mathrm{CADR}}{V} \tag{12}$$

The difference between $\lambda_{v,1}$ and $\lambda_{v,2}$, $\Delta\lambda_v$ (h^{-1}), represents the number of outdoor air changes per hour that ventilation can be reduced by, owing to the presence of the biowall, without increasing the TVOC concentration indoors. There were instances in the Monte Carlo simulation where the CADR was high enough such that a negative value for $\lambda_{v,2}$ was obtained. In these cases, $\lambda_{v,2}$ was set equal to zero, because a negative ventilation rate is not possible. Consequently, this implies that these cases would produce a C_2 value less than C_1, resulting in an improved TVOC concentration despite operating the building without ventilation.

The energy saved on ventilation in Scenario 2 is simply the energy needed to condition $\Delta\lambda_{v,}$, which can be calculated from thermal and humidity differences between the outdoor and

indoor air. These differences vary both spatially across the globe and temporally throughout a year and a day, depending on the building's location and weather conditions.

2.2.2. Climate modeling

Each iteration of the Monte Carlo simulation was run for multiple locations to represent the range of climates conditions found across the U.S. and assess the impact of climate on biowall cost effectiveness. The simulated locations spanned 16 cities specified by Deru et al. (2011) within the continental U.S., with each being representative of one of the 16 climate zones illustrated in Figure 8 and specified by the International Energy Conservation Code (IECC) and ASHRAE 90.1 (2016). The locations and their IECC climate zones are listed in Table 1, grouped by their broader climate characteristics defined by the Building America program (Beachler et al., 2010). Also in the table are metrics describing the climactic conditions of each location, including degree-days (DD), calculated with a base of 18 °C from typical meteorological year version 3

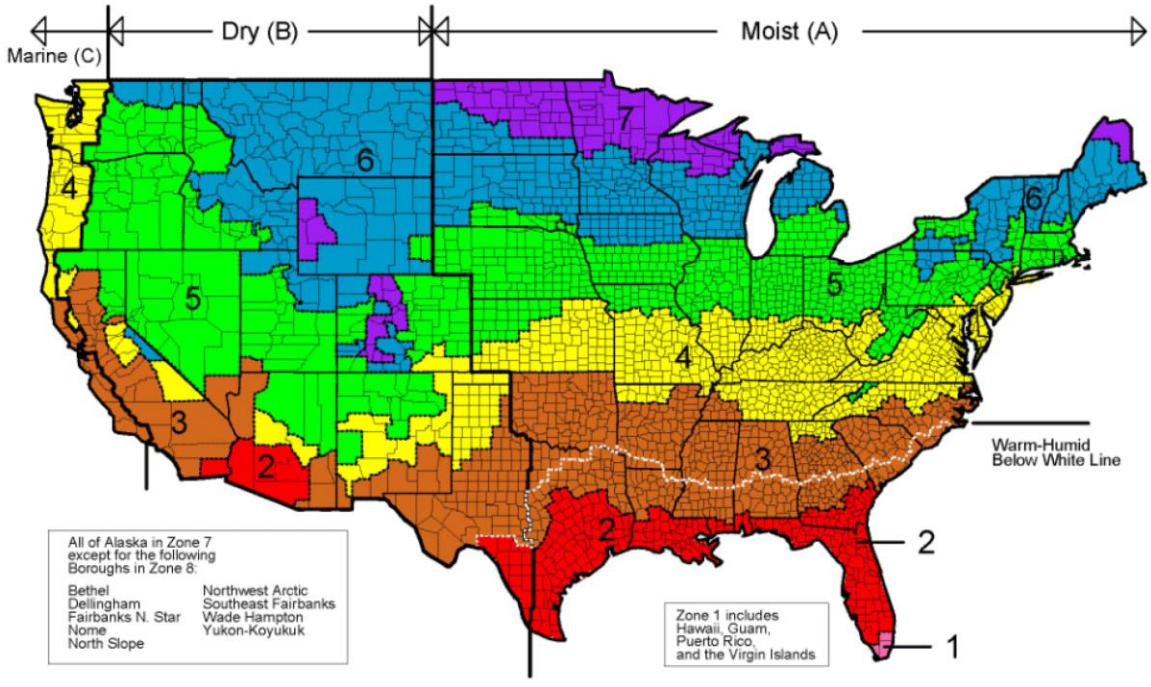

Figure 8 Climate zone delegation by county in the contiguous U.S. (Image from Deru et al., 2011.)

(TMY3) data files, and the median degree-hour (DH) values, defined in the following paragraphs, which resulted from the Monte Carlo simulation. Each Monte Carlo operation generated 100,000 instantiations, with each operation simulated across each of the 16 climate zones, resulting in 1,600,000 simulations occurring in total.

Both sensible and latent loads were considered when developing the climate models for each location. All loads were modeled with degree hours (DH). Similar to the better-known degree day (DD), a DH is a deviation in temperature of 1 degree from a balance temperature (T_{bal}) over the course of one hour, here in units of (°C·h). DHs were computed only for hours during which the HVAC system was operational. This approach allowed us to tailor DH values to any balance temperature and HVAC schedule. As a result, each modeled location of each iteration of the simulation produced unique DH results representative of the thermal loads a typical range of buildings would experience.

Annual heating DHs (HDH) and cooling DHs (CDH) over the course of a typical year were determined separately via the following equations:

$$\text{HDH} = \sum_{i=\text{day 1}}^{\text{day 365}} \sum_{j=t_{\text{on}}}^{t_{\text{off}}} \left(T_{\text{bal}} - T_{i,j}\right)_{+} \tag{13}$$

$$\text{CDH} = \sum_{i=\text{day 1}}^{\text{day 365}} \sum_{j=t_{\text{on}}}^{t_{\text{off}}} \left(T_{i,j} - T_{\text{bal}}\right)_{+} \tag{14}$$

where $T_{i,j}$ (°C) is the dry-bulb temperature of the outdoor air, taken from TMY3 data files for each representative city, for day i and hour j; and t_{on} and t_{off} (h) are the times of the day (in hours after midnight) that the HVAC system is turned on and off respectively. The "+" symbol denotes that only positive values are considered within the summation.

Latent loads were also considered, but only during times at which cooling was being provided by the HVAC system. Analogous to DHs, latent enthalpy hours (LEH) were used to model latent loads, where one LEH represents a deviation in latent enthalpy of 1 kJ/kg over the course of one hour, here in units of kJ·h/kg (Huang et al., 1986). LEHs over the course of a typical year were determined for each run by:

$$\mathrm{LEH} = H_{\mathrm{vap}} \sum_{i=\mathrm{day}\ 1}^{\mathrm{day}\ 365} \sum_{j=t_{\mathrm{on}}}^{t_{\mathrm{off}}} \left(W_{i,j} - W_{\mathrm{set}}\right)_{+} \tag{15}$$

where H_{vap} (kJ/kg) is the latent heat of vaporization of water, equal to approximately 2205 kJ/kg; W_{set} is the base humidity ratio determined from the relative humidity (RH) setpoint; and $W_{\mathrm{i,j}}$ is the humidity ratio of the outdoor air, determined from the RH taken from TMY3 data files for each representative city, for day *i* and hour *j*. This calculation was only done for hours where $T_{\mathrm{i,j}}$ was

Table 1 Locations simulated and their climate zones, base 18°C annual HDD and CDDs, and median annual HDHs, CDHs, and LEHs from the Monte Carlo simulation.

Building America climate zone	IECC climate zone	Location	Typical base 18°C DDs (K·d)		Median DHs from energy simulation (K·h)		
			HDD	CDD	HDH	CDH	LEH
Hot-humid	1A	Miami	2494	119	1585	45325	105117
	2A	Houston	1755	894	12888	34074	71981
Hot-dry/	2B	Phoenix	2775	657	9576	52015	12630
Mixed-dry	3B-coast	Los Angeles	326	751	10157	7284	22110
	3B	Las Vegas	1992	1322	19008	38969	3373
	4B	Albuquerque	849	2427	36739	17923	4540
Mixed-humid	3A	Atlanta	1131	1622	25070	22566	40352
	4A	Baltimore	804	2553	40174	16196	29723
Marine	3C	San Francisco	132	1667	24018	3138	4711
	4C	Seattle	177	2644	41341	4042	4050
Cold/Very cold	5A	Chicago	599	3524	56423	12409	22632
	5B	Boulder	552	3362	51273	12437	2050
	6A	Minneapolis	528	4276	69604	10727	17876
	6B	Helena	330	4286	68106	7344	665
	7	Duluth	186	5289	85871	4162	7806
	8	Fairbanks	98	7192	118271	2175	1073

greater than T_{bal}, which formally applied the constraint that dehumidification only be considered during times of cooling.

2.2.3. Energy savings

In addition to just HDHs, CDHs, and LEHs, energy loads imposed by conditioning ventilation air also depend on the amount of air ventilated and the properties of the HVAC equipment. This work assumes that heating will be accomplished by a natural gas fired furnace, and cooling by an electric chiller. The energy that is saved on conditioning ventilation air due to the $\Delta\lambda_v$ reduction in air exchange was modeled by Equations 16 and 17 for heating and cooling, respectively:

$$E_h = \frac{1}{\eta_h}\frac{\Delta\lambda_v}{3600}\rho V c_p(\mathrm{HDH}) \tag{16}$$

$$E_c = \frac{1}{\mathrm{COP}}\frac{\Delta\lambda_v}{3600}\rho V\left(\left(c_p(\mathrm{CDH})\right) + \mathrm{LEH}\right) \tag{17}$$

where E_h and E_c (kWh/y) are the energies saved on heating and cooling respectively; ρ (kg/m^3) is the density of air; c_p (kJ/kg·°C) is the specific heat of air; η_h is the efficiency of the heating furnace; and COP is the coefficient of performance of the chiller.

2.2.4. Biowall loads

The annual energy input that the biowall requires for its operation was modeled by the following equation:

$$E_b = 365 \cdot A_b\left((\mathrm{LPD} \cdot h_L) + \left(\mathrm{FPD} \cdot (t_{off} - t_{on})\right) + (\mathrm{PPD} \cdot 24)\right) \tag{18}$$

Where E_b (kWh/y) is the annual energy consumed by the biowall; h_L (h) represents the number of lighting hours per day (i.e., the amount of time in hours each day that the biowall is supplemented by artificial lighting); and LPD, FPD, and PPD (kW/m^2) are the lighting, fan, and pump power densities, each normalized by the area of the biowall. Respectively, they represent the amount of lighting power the biowall needs, the fan power needed to pull air through the biowall, and the pump power needed to recirculate water through the biowall. The PPD was multiplied by 24 hours per day as the pump was modeled as being on continuously, under the assumption that the plants living on the wall need a continuous supply of water regardless of the time of day and building occupancy. The fan was modeled as being on only when the HVAC system is operational, hence FPD was multiplied by the difference between t_{off} and t_{on}. And the biowall was modeled as being artificially lit for h_L hours each day, which was considered to vary on a case-by-case basis depending on the amount of natural sunlight provided to the biowall.

In addition to E_b, which is a purely electrical load, the biowall also imposes a water load on the building. Water circulating from the reservoir to the top of the wall and down the root media evaporates from the plants, the root media, and the surface of the reservoir itself. Fresh water also periodically replaces the more stagnant water in the reservoir so it does not harbor bacteria. These two factors combine to yield a total water replacement rate, Q_w (gal/h).

2.2.5. Varied input parameter distributions

All parameters were modeled as probability distributions and are presented in Table 2. We categorized three distinct groups from which factors affect the biowall's performance. When able, parameters were defined by published distributions based on statistical data. For parameters where no statistical data reflecting realistic conditions exist, we relied on values used in previously published literature for analogous parameters.

Table 2 Definitions of the varied input parameter distributions, along with their units and shortened names used in the equations and text throughout this paper.

Group	Parameter	Short name	Units	Distribution			Ref.	Notes
				Type	J	k		
Building environment	Floor area	A_f	m^2	LN	1413	1.49	2	-
	Ceiling height	H_c	m	LN	3.67	1.12	2	-
	Indoor TVOC emission rate	E/V	$\mu g/h \cdot m^3$	LN	251.7	1.62	1	-
	Outdoor TVOC concentration	C_{out}	$\mu g/m^3$	LN	69.1	2.34	1	-
Building operation	Baseline ventilation AER	$\lambda_{v,1}$	h^{-1}	LN	1.21	2.71	2	-
	Balance temperature	T_{bal}	°C	N	18	1.08	-	-
	Relative humidity setpoint	RH_{set}	%	N	50	7.76	-	-
	Time HVAC on	t_{on}	h	U	0	8	-	-
	Time HVAC off	t_{off}	h	U	18	24	-	-
	Coefficient of performance	COP	-	N	3	1	3	-
	Heating efficiency	η_h	-	N	0.8	0.2	3	-
Biowall design & operation	Relative biowall size	R	-	LN	0.026	2.27	-	-
	Flux through biowall	v_b	m/s	LN	0.125	2.27	-	-
	Biowall removal efficiency	η_b	-	N	-	-	-	d
	Biowall lighting hours	h_L	h/d	U	0	24	-	-
	Lighting power density	LPD	kW/m^2	LN	0.1	2.44	4	a
	Pump power density	PPD	kW/m^2	LN	0.01	2.44	4	a
	Fan power density	FPD	kW/m^2	LN	0.01	2.44	4	a
	Water replacement rate	Q_w	gal/h	LN	0.63	2.44	-	a, c
	Biowall maintenance cost	M_b	$\$/m^2 \cdot y$	LN	102	2.44	-	a, c
Utilities	Electricity price	P_e	¢/kWh	GMD	-	-	-	e
	Natural gas price	P_g	¢/kWh	LN	3.65	1.27	-	-
	Water price	P_w	¢/gal	LN	0.5	1.87	-	b

LN = lognormal distribution, j = geometric mean (GM), k = geometric standard deviation (GSD).
N = normal distribution, j = mean, k = standard deviation (SD).
U = uniform distribution, j = min, k = max.
GMD = Gaussian mixture distribution.
a. assumed the 99% confidence interval is bounded by the GM x/÷ 10.
b. assumed the 99% confidence interval is bounded by the GM x/÷ 5.
c. j term derived from Drexel's biowall.
d. $j = 0.564e^{-7.921v_b}$, $k = 0.181e^{-5.573v_b}$
e. 67.8% ~N(9.36, 1.152), 32.2% ~N(14.04, 3.152).
1. Rackes and Waring, 2013
2. Rackes and Waring, 2015
3. Rackes and Waring, 2017
4. Nedlaw Living Walls, 2017

The typical floor area served by the HVAC system, the ventilation air exchange rate, ceiling height, and indoor volumetric TVOC emission rates were set by published distributions reflecting realistic conditions in office buildings across the U.S. (Rackes and Waring, 2013; Rackes and Waring, 2015). The building volume was modeled as the product of the floor area and ceiling height, and the distribution of ambient outdoor TVOC concentrations is reflective of general conditions across the U.S. (Rackes and Waring, 2013).

It was assumed that the HVAC system would be operational for anywhere between nine and 24 hours per day, accounting for a range of building functions. The hours of the day that the HVAC system turns on and off were defined as uniform distributions. The efficiencies of heating and cooling equipment were defined by distributions taken from Rackes and Waring (2017).

Distributions for the relative biowall size, *R*, the air flux through the biowall, and TVOC removal efficiency were determined from the process described in Section 2.1. Nedlaw Living Walls provides typical values for LPD, PPD, and FPD on their website. These values were used as GMs of our lognormal distributions, and the GSDs were set so that the 99% confidence interval was bounded by a factor of 10 less and greater than the GM. The hours per day that biowall lighting were turned on was also varied, following a uniform distribution ranging from always on to always off. Cases where the lighting is always on would apply to conditions where the biowall receives little to no daylight, and cases where the lighting is always off would apply to conditions where the biowall receives perfect daylighting

Neither the water replacement rate nor the cost of biowall maintenance have precedents in past literature, or a suggested value from a third party. Instead, we used information about the functioning biowall at Drexel University to back-calculate area-normalized values for these two parameters. We assumed that the value for Q_w was typical, so we set it as the GM of its distribution, and again defined the GSD such that the 99% confidence interval was bounded by a factor of 10 less than and greater than the GM. For maintenance cost, M_b, in case what Drexel University incurs a larger than typical, we assumed the calculated value to be in the 75^{th} percentile. The GM was calculated based on that set 75^{th} percentile value.

For utility prices, we considered commercial sector retail prices for electricity (US EIA, 2016b) and natural gas (US EIA, 2016c) across all U.S. states, from 2005 to 2014, weighted by each state's total consumption (US EIA, 2016d; US EIA, 2016e), to which distributions were fit. The data for electricity prices were bimodal, and lognormal for the price of natural gas. No comprehensive collection of data representing utility prices of water was found when generating

distributions for this work. Water pricing, based upon various municipality's websites, is often bracketed by consumption and tiered based upon pipe size, rather than a linear relationship per gallon. We estimated that a nationally representative distribution would be lognormal, whose GM would fall near 0.5 cents/gal. A large GSD, which was designated such that the 99% confidence interval was bounded by a factor of 5 less than and greater than the GM, accounted for the low precision of our estimate.

3. RESULTS

This section presents the impacts of biowall operation from four perspectives. First, we assess its effectiveness as an indoor air cleaner considering TVOC concentrations. We then assess the potential of using the air-cleaning impacts of the biowall to reduce the outdoor air ventilation rate without an increase in indoor TVOC levels. These first two considerations stemmed from our main analysis: a detailed presentation of both the calculated energy and cost implications of using a biowall to reduce ventilation. Finally, we used statistical analysis techniques to help analyze the results as well as to create a linear model which predicts the energy and cost outcomes of

Table 3 Names and units of varied parameters, along with select percentiles.

Short name	Units	p5	p25	Median	p75	p95
A_f	m^2	739	1083	1415	1852	2714
H_c	m	3.05	3.40	3.67	3.96	4.42
E/V	$\mu g/h \cdot m^3$	113	182	252	349	555
C_{out}	$\mu g/m^3$	17.1	39	69.5	123	281
$\lambda_{v,1}$	h^{-1}	0.234	0.62	1.21	2.37	6.25
T_{bal}	°C	16.2	17.3	18.0	18.7	19.8
RH_{set}	%	37.2	44.7	50.0	55.2	62.6
COP	-	1.36	2.33	3.00	3.68	4.65
η_h	-	0.454	0.638	0.760	0.867	0.968
R	-	6.75E-03	1.49E-02	2.60E-02	4.53E-02	0.100
v_b	m/s	3.23E-02	7.19E-02	0.125	0.218	0.481
η_b	-	8.95E-03	8.19E-02	0.189	0.320	0.519
h_L	h/d	1.20	5.97	12.0	18.0	22.8
LPD	kW/m^2	2.28E-02	5.46E-02	9.96E-02	0.181	0.431
PPD	kW/m^2	2.30E-03	5.50E-03	1.00E-02	1.82E-02	4.27E-02
FPD	kW/m^2	2.31E-03	5.47E-03	1.00E-02	1.83E-02	4.33E-02
Q_w	gal/h	0.144	0.345	0.628	1.15	2.74
M_b	$\$/m^2 \cdot y$	23.9	56.2	103	188	451
P_e	¢/kWh	7.80E-02	9.00E-02	0.100	0.127	0.159
P_g	¢/kWh	2.46E-02	3.10E-02	3.65E-02	4.28E+02	5.14E-02

operating a biowall in a building, given known parameters. Table 3 summarizes the input parameters after the Monte Carlo sampling.

3.1. Biowall Effectiveness

The dimensionless effectiveness of any air cleaner in a particular building can be measured by how well it cleans the air compared to the building's ventilation air exchange rate. This metric is quantified by:

$$\Gamma = 1 - \frac{\lambda_{\mathrm{v},1}}{\lambda_{\mathrm{v},1} + \frac{\mathrm{CADR}}{V}} \tag{19}$$

where Γ (-) is effectiveness, and is computed for the baseline ventilation rate of, $\lambda_{\mathrm{v},1}$. Effectiveness can range from 0 to 1, scaled such that when $\Gamma = 0$ the air cleaner has no impact on IAQ, when $\Gamma = 1.0$ air exchange removal has no impact on IAQ (i.e., there is no ventilation), and when $\Gamma = 0.5$ the air cleaner and ventilation have equal impacts. While effectiveness is not a direct measure of potential energy savings, it is used here as a proxy for it, under the assumption that ventilation will be reduced to maintain the same IAQ as for baseline conditions.

To gain insight into the impact that relative biowall size has on effectiveness, we ran a Monte Carlo operation with inputs nearly identical to those described in Table 2, but *R* was run as a uniform distribution across a wide range of plausible values. We then proceeded to calculate effectiveness via Equation 19. For these Monte Carlo results, Figure 9 shows the plot of Γ versus *R* (note the log-scale on the *x*-axis). Also denoted in the figure are the bounds (99% confidence interval) and median value of *R* used in the energy simulation as defined in Table 2. This figure shows span of likely Γ values at any *R*. These results are in agreement with intuition, such that a larger biowall is more impactful than a smaller one.

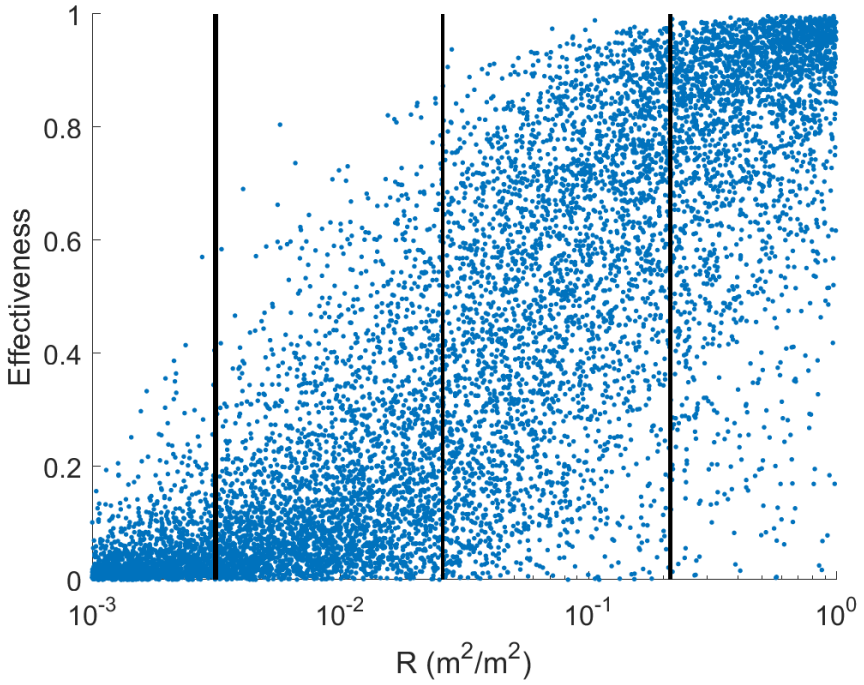

Figure 9 Scatter plot of Effectiveness and *R* combinations over a uniform distribution of *R*. Median and 99% confidence interval bounds of *R* used in energy simulation are also plotted.

Figure 10 is essentially a quantification of the scatter plot shown in Figure 9. It shows the effectiveness that can be expected, along with its variability, for different relative biowall sizes. Here, all the data are split into evenly log-spaced bins based on *R*, represented as the seven stacked bars in the figure. Each bar is split into segments which represent evenly spaced ranges of values for Γ. The portion of a particular segment accounts for the fraction of instances the effectiveness calculation fell into the range of that segment within its *R* bin. The median value of *R* from the Monte Carlo was 0.026 (section 2.1.4), equivalent to $10^{-1.59}$, which is located near the center of the fourth bar. As previously stated, Nedlaw Living Walls recommends an *R* of 0.01, and the third bar is centered about this value. At more extreme values of *R*, the biowall is nearly guaranteed to be either negligibly effective, or render ventilation useless (bear in mind, this is from a TVOC perspective only). Around median values of *R*, other parameters have more relative influence then *R*, and Γ has a nearly equal likelihood of falling anywhere between 0 and 1.

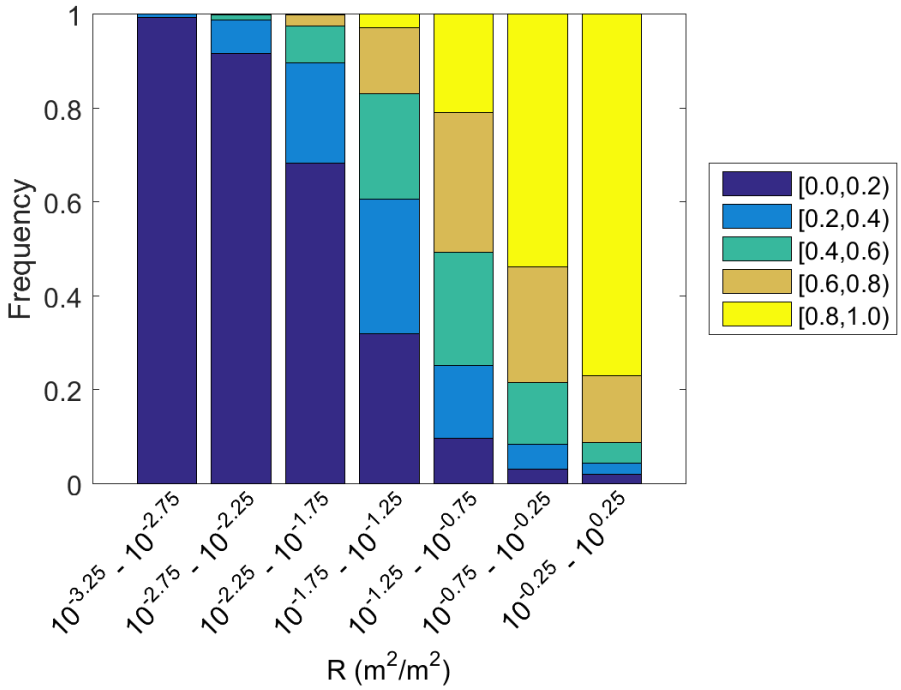

Figure 10 Stacked bar chart where the bars differentiate bins in *R*, and stacked segments represent fraction of total bar where effectiveness falls into the range denoted in the legend.

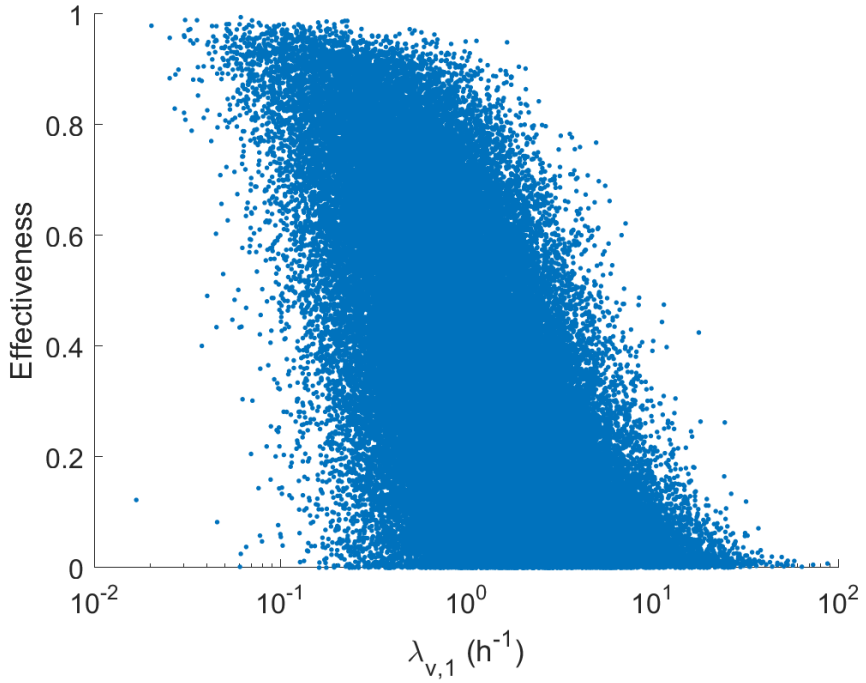

Figure 11 Scatter plot of Effectiveness and $\lambda_{v,1}$ combinations.

Effectiveness is also inversely proportional to the baseline AER. This is because, in accordance with Equation 19, a larger CADR would be required of an air cleaner to achieve the same effectiveness impact at a higher baseline ventilation rate. This relationship produces a nearly linear, albeit with large variability, relationship (excluding regions of effectiveness near its bounds of Γ at 0 and 1) between the $\log_{10}(\lambda_v)$ and Γ, as shown in Figure 11. From analyzing these factors, it becomes apparent that a biowall is a more effective air cleaner for buildings with combinations of larger relative sizes in the building and lower baseline ventilation rates.

3.2. Ventilation Reduction

We defined the potential reduction in ventilation (pRed), expressed as a percentage, as

$$\text{pRed} = 100\left(1 - \frac{\lambda_{v,2}}{\lambda_{v,1}}\right) \tag{20}$$

which represents the amount that a biowall will allow ventilation to be reduced without resulting in increased TVOC levels (per Section 2.2.1, the $\lambda_{v,2}$ was calculated so that TVOC concentration C_2 remained equal to C_1). In other words, a pRed of 0% means that $\Delta\lambda_v$ was equal to zero. A pRed of 100% means that $\Delta\lambda_v$ was equal to $\lambda_{v,1}$ (i.e., Scenario 2 does not require ventilation).

Figure 12 presents pRed values across a range of binned R values, as was done in Figure 10 in the previous section. Within the fourth bar (i.e., the median value of R), the plurality of cases (roughly 35%) results in 100% ventilation reduction (i.e., no ventilation is necessary). In these cases, TVOC levels can equal or improve upon baseline conditions (i.e., $C_2 \leq C_1$). However, about 65% of these cases still require ventilation, for which TVOC levels remain unchanged from baseline conditions (i.e., $C_2 = C_1$). Also notable is the relationship between pRed and Γ. The threshold for a 100% reduction in ventilation occurs about where $\Gamma = 0.5$ (on Figure 10). This is

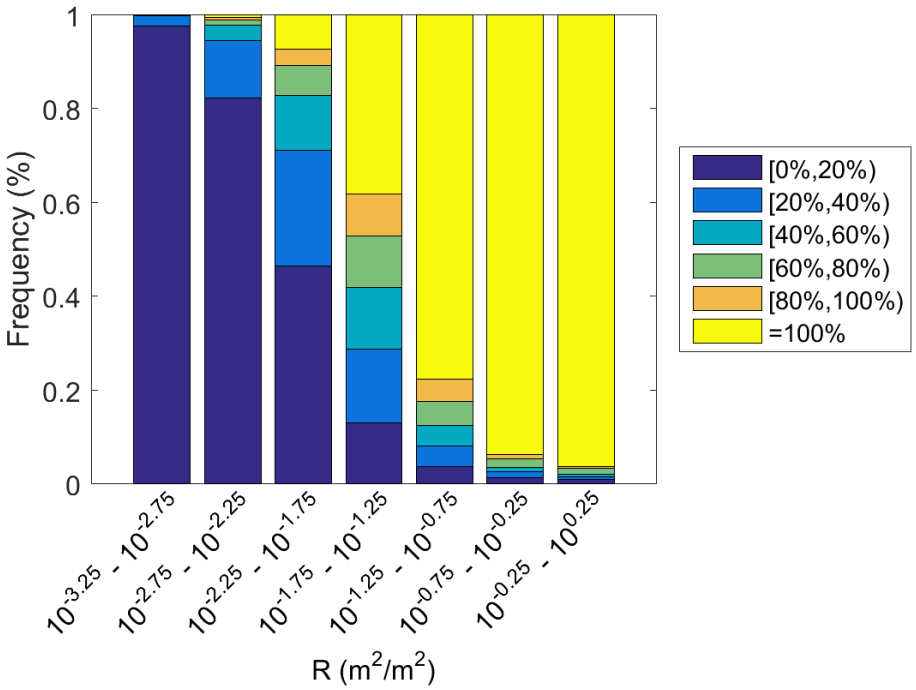

Figure 12 Stacked bar chart where the bars differentiate bins in *R*, and stacked segments represent fraction of total bar where pRed falls into the range denoted in the legend.

consistent with the definition of $\Gamma = 0.5$ meaning that the air cleaner is now as impactful as $\lambda_{v,1}$, so air cleaning can fully replace ventilation without seeing an increase in TVOC concentration.

3.3. Energy, Cost, and Climate

Each of the 100,000 instantiations of the Monte Carlo simulation, which represents one particular combination of a building and biowall, was simulated over all 16 climate zones separately, per Section 2.2.2. This operation allowed for a unique response to varying climates to be captured independently of other variables. We analyze six relevant outputs: (1) energy savings and (2) monetary savings from ventilation reduction, (3) energy costs and (4) monetary costs due to biowall loads, and net change in (5) energy consumption and (6) operating cost.

Energy type (i.e. electricity or gas) was ignored when considering raw energy consumption, such that the total energy saved per year, E_v (kWh/y), for each modeled location is

simply the sum of E_c and E_h. Net reduction in energy consumption, E_{net} (kWh/y), was the difference between the energy load of the biowall, E_b, and E_v. A positive value implies that the user saved energy due to the operation of the biowall, while a negative value implies that operating the biowall increased energy consumption.

However, energy type was not ignored when assessing operational cost. Electricity and gas prices per kWh were multiplied by E_c and E_h respectively to yield the cost of both. Their sum represents the total annual HVAC savings, S_v (\$/y), provided by the biowall. The operating cost of the biowall, S_b (\$/y), has three separate components: electrical loads, water loads, and maintenance. The electrical cost component is the product of E_b and the price of electricity. The cost component due to water loads is the product of the Q_w and the price of water. The estimate of maintenance cost, M_b, for replacement of the plants on the biowall as well as general upkeep, determined as was laid out in Section 2.2.5, was used for the final cost component. Net change in the building's operating cost, S_{net} (\$/y), is the difference between S_v and S_b.

Values of E_b, S_b, and their components from the Monte Carlo simulation were not varied from one climate zone to another. Table 4 presents the median values of these parameters. In Table 5, median values of the remaining climate-dependent outcomes are presented. In the majority of cases throughout all modeled locations, the energy load imposed by the biowall is lower than the energy saved on conditioning ventilation air, while the cost of operating the biowall is greater than the money saved on conditioning ventilation air. This discrepancy can be mostly attributed to the high maintenance cost required to replace and upkeep the plants on the wall.

Table 4 Median annualized energy loads and cost components of the biowall.

Load	Usage (kWh/y)		Expense (\$/y)
Lights	12970		1374
Pump	3223		340
Fan	2249		237
Water	-		1009
Maintenance	-		3793
E_b =	18450	S_b =	6753

Intuition, as well Equations 16 and 17 for ventilation energy savings, tells that the potential to save energy increases as climate becomes less temperate. In more extreme climates, where the costs of conditioning are higher, decreasing a set amount of conditioned air has higher value. In cities where the thermal characteristics of outdoor air are more similar to comfort conditions, conditioning is cheap, so reducing outdoor air intake has less value. Figure 13 illustrates this relationship, and considers energy saved on cooling separately from heating.

Despite considering both sensible and latent loads during cooling while considering only sensible loads during heating, Figure 13 makes clear that significantly more energy is saved in cold climates than is saved for equally hot climates. This discrepancy is traced to our assumption made on HVAC equipment: that heating is done using gas, whose efficiency is always less than 1.0, and that cooling is done by an electric chiller, whose efficiency varies about 3. While these results accurately reflect the majority of the U.S. office stock, buildings which use heat pumping

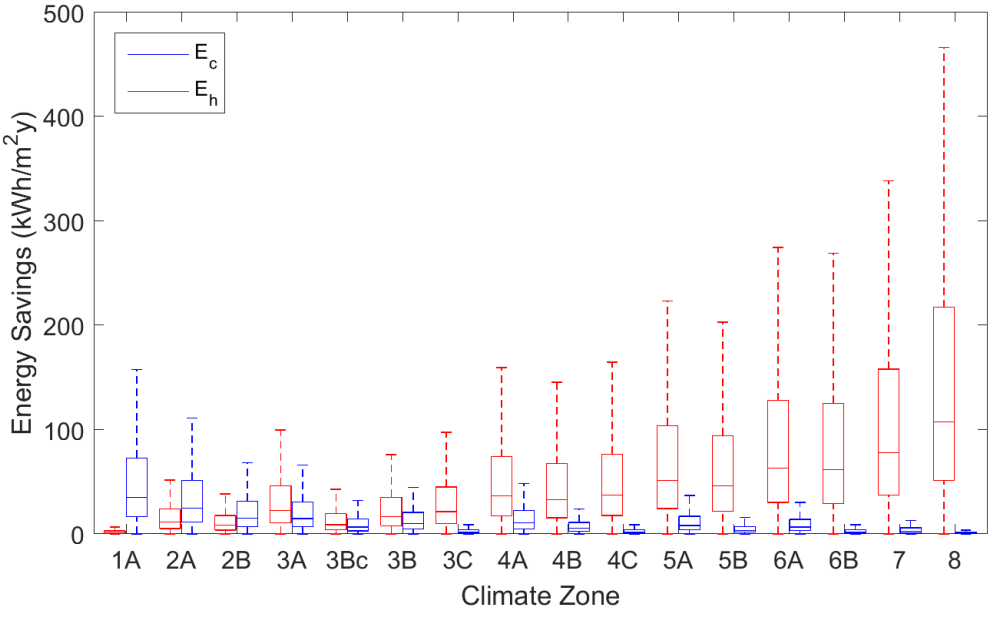

Figure 13 Energy saved by ventilation reduction on both heating and cooling, in red and blue respectively, normalized by the building footprint.

Table 5 Median annualized energy and cost savings on ventilation, as well as net changes in total energy consumption and operating costs. Results are normalized by the footprint of the building.

IECC climate zone	Energy (kWh/m²·y)				Savings ($/m²·y)	
	E_h	E_c	E_v	E_{net}	S_v	S_{net}
1A	1.35	35.00	36.73	15.96	3.76	-1.68
2A	11.40	24.73	37.55	16.70	3.12	-2.25
2B	8.34	15.20	24.66	6.29	1.98	-3.41
3A	22.50	14.70	38.84	17.76	2.50	-2.88
3B-coast	8.90	6.70	17.30	0.94	1.14	-4.44
3B	16.79	10.00	28.08	8.88	1.77	-3.68
3C	21.39	1.79	24.06	5.78	1.05	-4.59
4A	36.34	10.72	48.57	26.40	2.60	-2.81
4B	32.80	5.34	39.20	18.13	1.86	-3.58
4C	37.46	1.86	39.95	18.78	1.63	-3.85
5A	51.21	8.18	60.72	37.59	2.87	-2.54
5B	46.11	3.46	50.44	27.98	2.13	-3.28
6A	63.18	6.67	71.07	47.27	3.14	-2.28
6B	61.58	1.94	64.03	40.57	2.51	-2.89
7	78.02	2.78	81.40	57.10	3.22	-2.21
8	107.38	0.76	108.41	83.06	4.03	-1.52

in the winter will see heating savings reduce to the order of that seen for cooling savings presented in this work.

The median energy savings shown in Figure 13 are broken down in Table 5, which also shows ventilation energy and cost savings (E_v and S_v), as well as net energy and cost savings (E_{net} and S_{net}). Interestingly, while E_v and E_{net} are skewed toward cold climates, S_v and S_{net} are not. This is because the price of natural gas is cheaper than electricity so that, after accounting for efficiency, the cost per unit energy are roughly the same. Also clearly expressed in Table 5 is the significance of the latent portion of the cooling load. The E_c's of humid climate, whose climate zone is denoted with an "A," are consistently about 1.5-3 times higher than its corresponding dry climate zone number denoted with a "B". In marine climates, denoted with a "C," while the latent portions are on the order of humid climate zones A (see Table 1 in Section 2.2.2), their sensible cooling loads are significantly lower such that their E_c's are nearly an order of magnitude lower.

While a warm and a cold climate can produce similar annual savings (S_v or S_{net}), the profiles of when the savings occurs throughout the year are more unique. To show how these profiles vary between hot, mixed, and cold climates, from Table 1 in Section 2.2.2, Figure 14 shows how

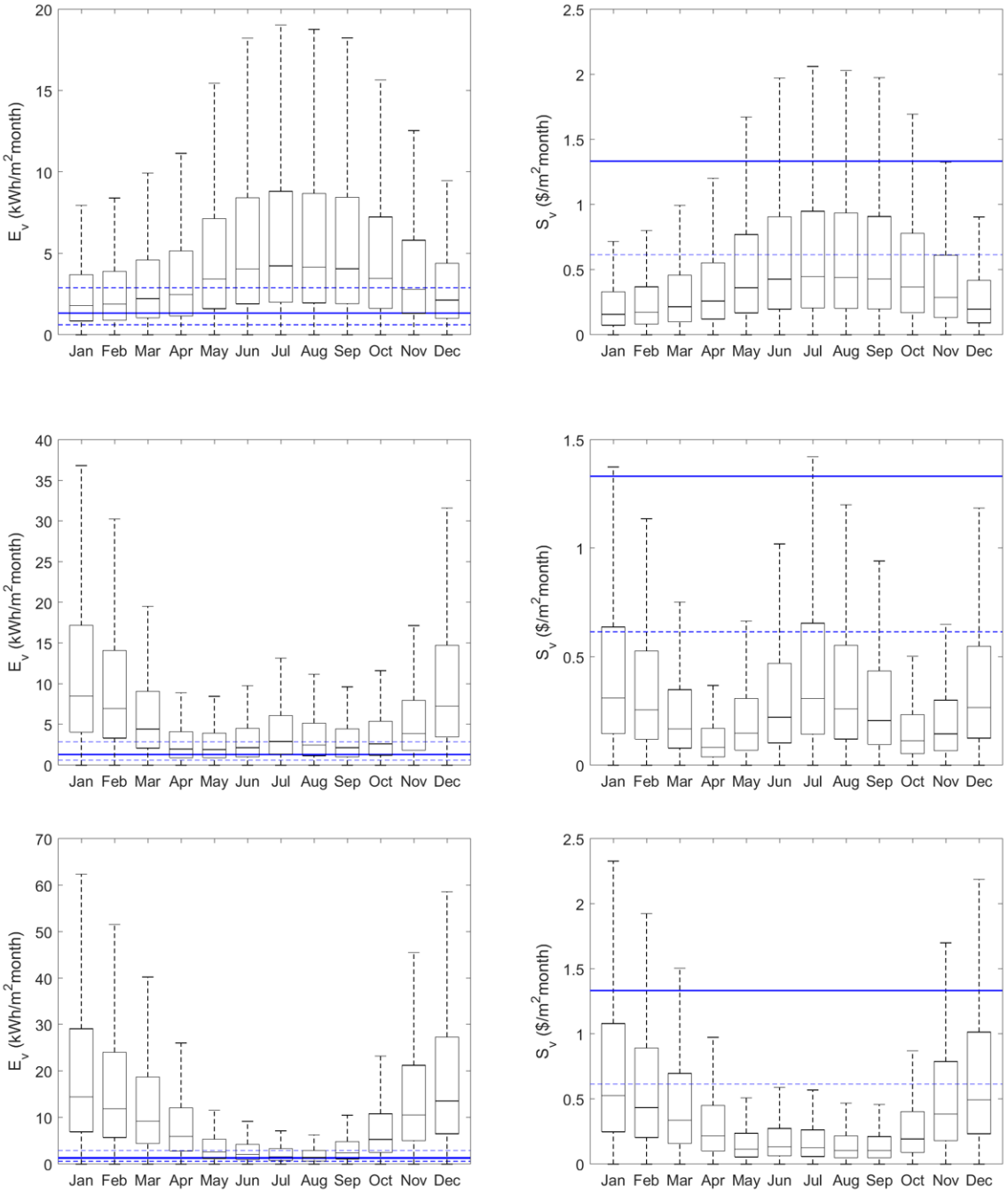

Figure 14 Monthly savings due to ventilation reduction of both energy (left) and US$ (right) for climate zones 1A (top), 4A (middle), and 7 (bottom). Median E_b and S_b's are overlaid as the solid horizontal lines, while the 25th and 75th percentiles are overlaid as the dotted horizontal lines.

E_v and S_v vary from month to month for climate zones 1A, 4A, and 7. Overlaying these boxplots are lines which represent the median, 25th, and 75th percentiles of E_b and S_b respectively. Plots

showing S_b omit the 75th percentile line as it lies well above the upper limits of the boxes. Captured in these illustrations are not only how savings is climate-dependent, but also how it is weather-dependent while the biowall loads are constant, as well as the larger savings in heating months than in cooling months.

In order to capture the impact of heating and cooling explicitly, rather than implicitly via climate zones, a contour plot of annual S_v was created by using median values for all parameters laid out in Equations 16, 17, and 18, but a continuous range of both heating and cooling DHs. With both axes claimed by HDH and CDH, in order to capture the impact of dehumidification, we correlated the median LEH to CDH from the 16 climates modeled in the Monte Carlo simulation. The correlations are linear per Figure 15, though two distinct trends are apparent that differentiate humid climates from dry ones. Consequently, this work shows one contour plot for S_v in humid climates for any combination of HDH and CDH (Figure 16), and another contour plot for

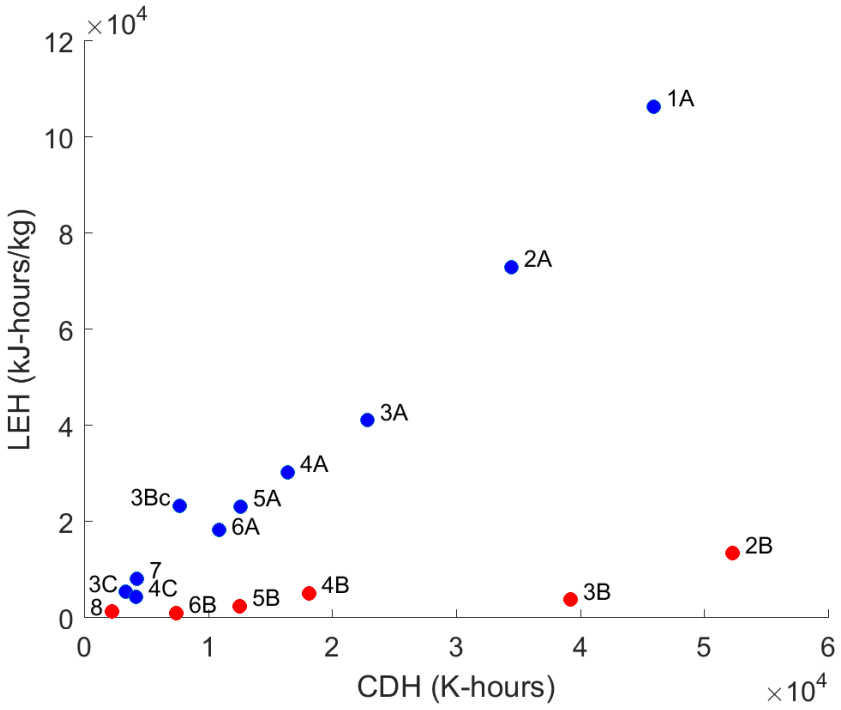

Figure 15 Two distinct correlations between CDH and LEH for humid (blue) and dry (red) climates.

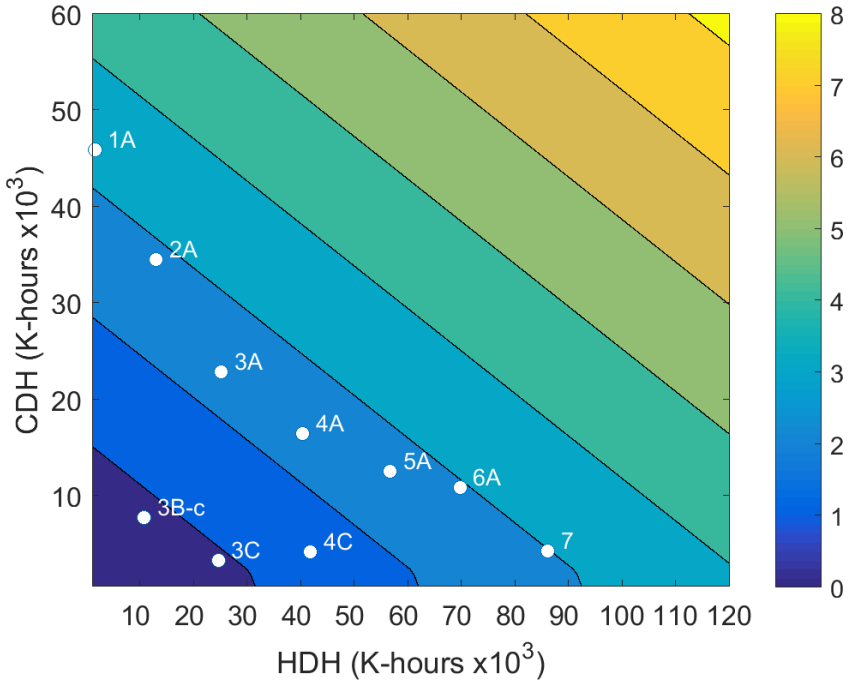

Figure 16 DH contour plot illustrating E_{net} (kWh/m^2·y) for humid climates.

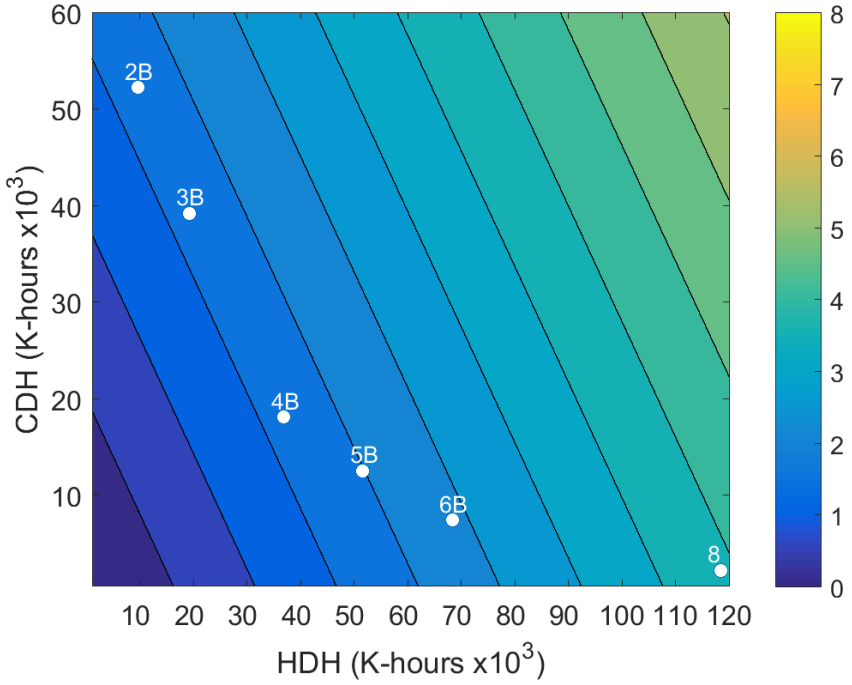

Figure 17 DH contour plot illustrating E_{net} (kWh/m^2·y) for dry climates.

dry climates (Figure 17). These figures present S_v in units of \$/m^2·y. Both contour plots have the same color scale. In accordance with Equations 16 and 17, energy savings vary linearly with DHs. Also shown on both plots are the discrete points at which the modeled climate zones fall. They fall in zones on the contour plot that match their S_v values reported in Table 5. These figures are illustrative in both showing how savings relate to climate, and also what reasonable values of energy savings can be achieved in a year at any climate in the U.S.

3.4. Statistical Analysis

We performed multiple linear regressions on the monetary outputs for two purposes: (1) to explore the parameters that are most influential on the outcome, and (2) to build a model which can accurately predict the outcome given a known set of parameters. For the first purpose, the explanatory model was generated by determining standardized regression coefficients (beta coefficients) for each independent variable (also referred to as a predictor). These coefficients, β_i, tell by how many SDs the dependent variable y will change for a single SD change in the predictor variable, x_i, per Equation 21:

$$\frac{y-\mu_y}{\sigma_y} = \beta_0 + \sum_i \beta_i z_i + \varepsilon = \beta_0 + \sum_i \beta_i \frac{x_i-\mu_i}{\sigma_i} + \varepsilon \tag{21}$$

where z_i is the standardized predictor variable; μ_i and σ_i are the arithmetic means and SDs of each predictor; and ε is an error term. A large β_i means that its corresponding x_i variable has a large effect on the outcome. The beta coefficients for S_{net} are presented in Table 6 in descending order. Therefore, from top to bottom, this table presents the parameters in order from most influential on the value of S_{net} to the least influential.

The predictors HDH, CDH, and LEH, and the dependent variables S_v and S_{net}, are two-dimensional 100,000-by-16 arrays, which span all 16 climate zones, while all other predictors are

one-dimensional 100,000-by-1 arrays which have no climate-dependent variation. For the regressions to proceed, all variable arrays must be the same size. We therefore converted the two-dimensional arrays to 100,000-by-1 one-dimensional arrays. We maintained the uniform representation of all 16 climate zones in the new data array by pulling its values for each row, m, from the m^{th} row and a randomly selected column n from the original two-dimensional array, where m spans from one to 100,000 and n spans from one to 16.

Beta values for S_v and S_b are also shown in Table 6. Values that have no effect on the particular outcome are omitted (e.g. COP does not affect the S_b nor does PPD affect S_v). Certain parameters (R, A_f, and P_e) impact both. The beta coefficients for these two parameters on S_{net} is a result of the difference between their positive influences on both S_v and S_b. Additionally, the small beta for T_{bal} is likely misleading. A lower balance temperature in a hotter climate leads to a higher baseline energy being spent on air conditioning, therefore a more energy savings. Similarly, a higher balance temperature in a colder climate also results in more savings. These two conditions cancel each other out for varying balance temperatures over all climates, resulting in a beta coefficient for T_{bal} near zero.

In addition to the explanatory model, a predictive linear model was also created for the purpose of predicting net savings based on the independent input variables. This was done for ventilation savings and biowall costs only, to maximize accuracy in light of the errors explained in the previous paragraph. The expected result for net savings can be determined by simply subtracting the S_b from the S_v values obtained through the predictive linear model. In this case, predictors are not standardized. Multiple linear regressions assume normality of the variables. We therefore log-transformed all lognormally distributed variables so that their transformed values have a normal distribution before the linear regression was performed. Because the dependent variables y considered here (S_v and S_b) most closely follow a lognormal distribution, they were also log-transformed, per Equation 22.

$$\ln y = c_0 + \sum_i c_i x_{N,i} + \sum_i c_i \ln(x_{LN,i}) + \varepsilon \tag{22}$$

Here, $x_{N,i}$ is the input for the *i*th predictor variable if it is either normally or uniformly distributed; $x_{LN,i}$ is the input for the *i*th predictor variable if it is lognormally distributed, and the c_i also presented in Table 6, are the regression coefficients. After the calculation for the RHS is done, simply take the exponential of the result to obtain the predicted outcome.

Table 6 Standardized and predictive regression coefficients for S_{net}, S_v, and S_v, as shown.

Dependent variable:		S_{net}	S_v	S_v	S_b	S_b
Predictor	Distribution	β_i	β_i	c_i	β_i	c_i
R	LN	-0.4717	0.1818	6.623E-01	0.6257	1.001E+00
M_b	LN	-0.3392	-	-	0.3713	4.942E-01
$\lambda_{v,1}$	LN	0.1956	0.3346	5.570E-01	-	-
LPD	LN	-0.1664	-	-	0.1840	2.314E-01
A_f	LN	-0.1406	0.1773	9.993E-01	0.2656	1.001E+00
HDH	-	0.1117	0.1958	1.448E-05	-	-
Q_w	LN	-0.0933	-	-	0.0979	1.661E-01
h_L	U	-0.0853	-	-	0.0903	2.205E-02
LEH	-	0.0798	0.1363	9.401E-06	-	-
COP	N	-0.0621	-0.1064	-1.818E-01	-	-
C_{out}	LN	0.0619	0.1038	2.275E-01	-	-
η_h	N	-0.0458	-0.0775	-9.135E-01	-	-
v_b	LN	-0.0429	-0.0723	-3.141E-01	-	-
CDH	-	0.0406	0.0766	1.354E-05	-	-
P_g	LN	0.0372	0.0612	5.843E-01	-	-
PPD	LN	-0.0301	-	-	0.0339	6.308E-02
E/V	LN	-0.0288	-0.0506	-2.165E-01	-	-
FPD	LN	-0.0213	-	-	0.0252	4.430E-02
P_e	LN	-0.0180	0.0461	4.338E-01	0.0490	3.488E-01
H_c	LN	0.0126	0.0202	3.112E-01	-	-
P_w	LN	-0.0087	-	-	0.0114	1.755E-01
T_{bal}	N	-0.0015	0.0007	6.648E-03	-	-
RH_{set}	N	-0.0005	0.0007	-1.469E-03	-	-
Intercept	-	-3.53E-15	-2.72E-16	5.27	1.21E-16	5.75
R^2 value	-	0.464	0.252	0.601	0.653	0.955

4. DISCUSSION

This section discusses the implications of the results of the Monte Carlo simulations contextualized by the differences between real systems and the underlying assumptions of the simulation. Also, as this technology is at least in part stemming from the green building movement, we

delve into a somewhat more abstract, but we argue necessary, discussion about how to characterize the sustainability of biowalls.

4.1. Sustainability

4.1.1. Definitions

Biowalls have many attributes, some of which are more sustainable than others. Broadly, and only recently, sustainability has been defined by the Brundtland Commission (or similarly by others) as meeting "the needs of the present without compromising the ability of future generations to meet their own needs" (World Commission on Environment and Development, 1987). In many circumstances, the contemporary hype around sustainability has made the word synonymous with efficiency, "green" building, or biophilia; but the existence of these does not necessitate sustainability. With the rise LEED certification, the word sustainability has become used more for marketability than it is used to accurately describe a system. Here, we consider sustainability through its more etymological dictionary definition, where "to sustain" can mean to indefinitely maintain, endure, or nourish. Thus, for the remainder of this work, we will define sustainability in the context of engineering as the ability to maintain the state of a system or process. By using this more rigorous definition and analyzing the biowall accordingly, we were able to gain meaningful insight into the performance of biowalls. This section intends to explore the sustainability of using a biowall as described throughout this work in two main contexts: (1) the process of biofiltration and (2) to biowall-building system, as well as their broader environmental impacts.

The best model available to base our engineered designs on are very often natural systems (e.g., Todd and Todd, 1994; Van der Ryn and Cowan, 1996). And Van der Ryn and Cowan (1996) suggest that the environmental problems we see impacting the natural world and technological and human problems we see plaguing the built environment are caused by their lack of integration with each other. They argue that many of these problems can be solved by ecological

design of our systems, which they define as a design which minimizes harmful impacts to the environment by integrating itself with living processes. By this definition, the prospect of the biowall is an ecological design.

4.1.2. Biofiltration process sustainability

What makes the process of biofiltration more sustainable than other air cleaning methods is the fact that biofilters convert air contaminants into biomass. As discussed in this work's introduction, filtration and adsorption simply transfer pollutants from the air stream to another medium. At some point in time, the pollutants must still be disposed of from that medium, and both pose the risk of reemission into the air stream. Alternatives that convert pollutants include oxidation, which can produce byproducts more harmful than initial pollutant, and photolysis (Guieysse et al., 2008). Biowalls, rather than merely transferring the original pollutant, convert it into useful biomass to be consumed by organisms living on the wall. Not only is turning waste into a resource a key feature of good ecological design (Bergen et al., 2001), but subsequently, the continuous conversion of VOCs means there will always be an adsorptive driving force (see the mechanisms of biofiltration discussion in the introduction). In other words, botanical purification does not require any changing of filters and provides its own adsorptive force without the input of external energy. This means it is better able to sustain its own process (i.e., be more sustainable) compared to other approaches.

4.1.3. Biowall system sustainability

But the inherent sustainability of an ideal botanical purification process does not necessarily translate into a sustainable biowall system. From looking at the results in Section 3.3, it is clear that the maintenance cost alone would make a biowall an unsustainable choice for the majority of consumers, with only 33.6% of instances from the Monte Carlo simulation having an $S_{net} > 0$. Even if the cost of plant maintenance was ignored, only ICEE climate zones 1, 2A, 5A, 6A,

7, and 8 would yield a positive S_{net} for the majority of cases. But a low maintenance biowall (i.e. small M_b and consequently S_b) with a small electrical load (E_b) can be a product of its design.

According to Drexel University's facilities manager, the main reason for the high cost of biowall maintenance is due to annual plant replacement (which was our motivation for assuming Drexel's M_b to be above the national median when defining our distributions). This high cost has been driven by a high rate of plant mortality, presumably due to inadequate lighting of the biowall. (The majority of the wall receives little to no direct solar radiation, so high-energy metal halide lighting was installed to compensate.) However, much of the lighting power is wasted, as the lights do not directly shine on the center of the wall. This is a case of poor design, where extra resources are expended without generating the desired outcome. The inherent sustainability of the biofiltration process has little significance when such an amount of energy and resources must be put in just to sustain a somewhat poorly functioning system.

Yet we do not believe that a biowall must inherently be attached to such a resource and energy-intensive form of life support in all cases, or most cases, if a good initial design is implemented. This fact is where one of the most prominent principles of ecological engineering and sustainable design comes into play: design for a site-specific context (Bergen et al., 2001). In the context of biowall design, this principle boils down to understanding the resources provided by the site and how accessible they are made by the building. A good design would be one where the building and the biowall are designed together, and the design of the building's glazing and orientation should maximize the biowall's exposure to sunlight. The biowall may not be a sustainable system if it is in a climate or even a particular location within a building where it does not have access to adequate natural light. Sufficient natural lighting via a sustainable design can eliminate the need for energy to be spent on artificial lighting. It can also reduce the rate of plant mortality and the need for maintenance. Reducing these two variables, the two largest components of S_b, can lead to both a reversal of the cost-effectiveness identified in this paper's simulation and a more truly sustainable biowall-building system from a cost perspective.

However, the sustainability of biowalls does not need to be reduced to cost only. The "triple bottom line" is the concept that one's bottom line is not measured exclusively by monetary profit, but also social and environmental impact. Not only do biowalls clean the air and/or reduce energy consumption, but incorporating green space into the built environment has been shown to have a positive impact on occupants' mental wellbeing (e.g. Raanaas et al., 2011). This phenomenon is known biophilia. Operational costs of the biowall might be offset for businesses by the productivity gains of working in a greener environment. Occupant happiness is also an aspect worth measuring, even if it lacks a hard cost component. Further psychological studies must be conducted to quantify these potential effects and better determine the triple bottom line of implementing a biowall in a workspace.

4.2 Model Limitations

One of the first assumptions made in this paper is that the entirety of IAQ will be assessed through the lens of VOCs only. There are many more pollutants which biowalls have no impact on, including ozone, carbon dioxide, particulate matter, etc. If ventilation were completely replaced with recirculating indoor air through a biowall, those other pollutants which are emitted indoors will likely accumulate to unhealthy levels. Therefore, this study does not recommend completely shutting down ventilation to use biofiltration alone. For ventilation to be eliminated, multiple air cleaners targeting all indoor air pollutants must be implemented. More plausibly, biofiltration can allow for ventilation to be reduced from $\lambda_{v,1}$ to minimum values specified by ASHRAE 62.1 (2010), or said minimum specifications might be reduced under the provision that adequate biofiltration is implemented. This could save energy while maintaining other classes of pollutants at reasonable levels.

Our model also implicitly considers ventilation air separately from recirculation air. This allowed us to simply look at savings on ventilation air only. However, ventilation and recirculation air are mixed before conditioning occurs in the AHU. This fact leads to error in our model under certain circumstances.

Recirculation air will nearly always be at a greater enthalpy than the conditioned air at T_{bal} and RH_{set}, due to the presence of internal gains from occupants and equipment. When outdoor air enthalpy is also greater than the target enthalpy (i.e., enthalpy at T_{bal} and RH_{set}) our model is accurate. This is because the sum of the energies needed to cool two streams of air (ventilation and recirculation separately, as our model's math implicitly depicts) is equal to the energy needed to cool the sum of the two streams of air (as actually occurs in an AHU).

When outdoor air enthalpy is less than the target, our model assumes heating is necessary. But in a real AHU, depending on the fraction of supply air that is made up of cool ventilation air and warm recirculation air, as well as the specific temperatures themselves, the mixed air enthalpy which will be conditioned may be greater than the target enthalpy. In this case, our model simulated heating when cooling would occur in reality.

Our model also neglects economizing. We assume that minimizing ventilation by recirculating biofiltered air is desirable in all weather conditions. But when conditioning ventilation air is cheaper than conditioning recirculation air, 100% ventilation air, or some increased fraction of ventilation air depending on the conditions, should be used under smart control strategies. The biowall, when economizing is in effect, spends energy as a part of E_b while contributing to no additional ventilation savings. The result, in our model, is an overestimation of energy savings, especially in temperate climates. Despite this error, we were able to demonstrate the poor cost-effectiveness of the biowall in these climate zones anyway without even considering economizing.

We also did not consider any change in cooling loads or system efficiency between scenario 1 and scenario 2. The biowall's artificial lighting may add to the sensible cooling load. It's

water circulation (Q_w) is partly necessitated by evapotranspiration to the indoor air. This will contribute to the latent cooling. We also did not model the possible outcome that due to ventilation reduction, the HVAC system might be downsized, resulting in increased system efficiency. Our primary reason for neglecting these in our model was due to the lack of known values for these parameters.

Additionally, this study's main purpose was to analyze the engineered systems related to buildings and biowalls, not their economics. While we have achieved a general idea of expected cost savings, as seen from Section 3.4, it is highly dependent on M_b, a parameter for which we have only been able to obtain a rather rough estimate for (see Section 2.2.5). Nor does this work consider upfront costs. In order to obtain this information and determine a return period, a separate economic feasibility study should be conducted.

4.3 Future Work

Biowalls are still a developing technology which require more study in order to be better understood. More extensive simulations should be run in analysis programs such as EnergyPlus, which can better model the mechanics in the AHU and economizing discussed previously. Field studies must also be conducted to verify the simulation results. More thorough cost-benefit analyses should also be conducted which include capital costs in addition to operational costs.

In addition to more thorough energy and cost studies, further research on the implications of biowall on IAQ and occupant wellbeing is necessary. For example, while biowall uptake of VOCs have been shown, plants have been shown to emit certain VOCs as well which can react with oxidizers such as ozone to produce secondary organic aerosols (Joutsensaari et al,. 2005). Biowalls may be a source of spore emissions, although Darlington et al. (2000) suggested the levels do not exceed common background ones. Psychological studies on biowalls' influence on occupant happiness and productivity due to biophilia must also be conducted. Biowalls and other air cleaning methods are not yet recognized by ASHRAE as an alternative to ventilation. A more

thorough understanding of biowalls' implications on IAQ may enable a shift in building codes, as the green building movement continues to demand higher IAQ and less expenditure of energy on ventilation.

5. CONCLUSIONS

Comprehensive Monte Carlo simulations were conducted to quantify and explore the energy savings potential and effectiveness of using biowalls as a ventilation alternative for controlling indoor VOCs in U.S. office buildings. This work also determined parameters which, if not fully representative of the range of operational biowalls in the U.S., represent target values based on the literature pertaining to biofiltration and laboratory biowalls.

We determined that air should be pulled through the biowall at a face velocity of about 0.125 m/s in order to maximize the CADR. This, however, will vary based upon the exact removal efficiency-velocity profile of the particular biowall constructed. A biowall will be more effective (as an air cleaner) in a building where the biowall to floor area ratio is large and the baseline ventilation rate is low.

Biowalls are typically designed so that they require a significant amount of energy to operate. Therefore, a net reduction in energy consumption can only occur when the energy saved on ventilation is greater than that used to maintain the biowall. The potential to save energy on ventilation is largely a function of climate. Where the climate is temperate and the cost to condition is low, replacing ventilation with recirculated biofiltered air has little value—and may even be more expensive when economizing can be done. In these cases, the cost to operate the biowall will be higher than that saved. In extreme climates where the cost of conditioning is high, reducing ventilation can save much more energy and money than is spent on the biowall. Energy savings are also influenced by the type of heating and cooling equipment used.

We also determined that net monetary savings is highly dependent on maintenance cost of the biowall, for which a good estimate does not yet exist as biowalls are an emerging technology. But with a good sustainable design which is based on ecological design principles, the cost and energy required to maintain and operate the biowall have the potential to approach insignificance. More field study and experimentation is required to better determine statistics which accurately represent the U.S. biowall stock. And more implementation in operational commercial buildings is required to obtain a better understanding of the costs and net savings associated with biowall operation.

LIST OF REFERENCES

AHSRAE 62.1. (2016). Ventilation for acceptable indoor air quality.

ASHRAE 90.1. (2016). Energy standard for buildings except low-rise residential buildings.

Baechler, M. C., Williamson, J. L., Gilbride, T. L., Cole, P. C., Hefty, M. G., & Love, P. M. (2010). *Building America best practices series: volume 7.1: guide to determining climate regions by county* (No. PNNL-17211 Rev. 1). Pacific Northwest National Laboratory (PNNL), Richland, WA (US).

Bergen, S. D., Bolton, S. M., & Fridley, J. L. (2001). Design principles for ecological engineering. *Ecological Engineering*, *18*(2), 201-210.

Chen, W., Zhang, J. S., & Zhang, Z. (2005). Performance of air cleaners for removing multiple volatile organic compounds in indoor air. *ASHRAE transactions*, *111*(1), 1101-1114.

Darlington, A. B., Chan, M., Malloch, D., Pilger, C., & Dixon, M. A. (2000). The biofiltration of indoor air: implications for air quality. *Indoor air*, *10*(1), 39-46.

Darlington, A. B., Dat, J. F., & Dixon, M. A. (2001). The biofiltration of indoor air: air flux and temperature influences the removal of toluene, ethylbenzene, and xylene. *Environmental science & technology*, *35*(1), 240-246.

Deru, M., Field, K., Studer, D., Benne, K., Griffith, B., Torcellini, P., ... & Yazdanian, M. (2011). US Department of Energy commercial reference building models of the national building stock.

Fisk, W. J. (2000). Health and productivity gains from better indoor environments and their relationship with building energy efficiency. *Annual Review of Energy and the Environment*, *25*(1), 537-566.

Fisk, W. J., Black, D., & Brunner, G. (2012). Changing ventilation

rates in US offices: Implications for health, work performance, energy, and associated economics. *Building and Environment*, *47*, 368-372.

Guieysse, B., Hort, C., Platel, V., Munoz, R., Ondarts, M., & Revah, S. (2008). Biological treatment of indoor air for VOC removal: Potential and challenges. *Biotechnology Advances*, *26*(5), 398-410.

Huang, Y. J., Ritschard, R., Bull, J., & Chang, L. (1986). *Climatic indicators for estimating residential heating and cooling loads* (No. LBL-21101; CONF-870101-6). Lawrence Berkeley Lab., CA (USA).

Jones, A. P. (1999). Indoor air quality and health. *Atmospheric environment*, *33*(28), 4535-4564.

Joutsensaari, J., Loivamäki, M., Vuorinen, T., Miettinen, P., Nerg, A. M., Holopainen, J. K., & Laaksonen, A. (2005). Nanoparticle formation by ozonolysis of inducible plant volatiles. *Atmospheric Chemistry and Physics*, *5*(6), 1489-1495.

Klepeis, N. E., Nelson, W. C., Ott, W. R., Robinson, J. P., Tsang, A. M., Switzer, P., ... & Engelmann, W. H. (2001). The National Human Activity Pattern Survey (NHAPS): a resource for assessing exposure to environmental pollutants. *Journal of Exposure Science and Environmental Epidemiology*, *11*(3), 231.

Lomborj, B. (2002). The Skeptical Environmentalist. Cambridge University Press,

Cambridge, MA, p. 182

Malhautier, L., Khammar, N., Bayle, S., & Fanlo, J. L. (2005). Biofiltration of volatile organic compounds. *Applied microbiology and biotechnology*, *68*(1), 16-22.

Nedlaw Living Walls. (n.d.) Energy conservation and related cost savings with indoor air biofilters. http://www.nedlawlivingwalls.com/wp-content/uploads/Energy-Conservation-and-Related-Cost-Savings-with-Indoor-Air-Biofilters.pdf (accessed June 11, 2017).

Raanaas, R. K., Evensen, K. H., Rich, D., Sjøstrøm, G., & Patil, G. (2011). Benefits of indoor plants on attention capacity in an office setting. *Journal of Environmental Psychology*, *31*(1), 99-105.

Rackes, A., & Waring, M. S. (2013). Modeling impacts of dynamic ventilation strategies on indoor air quality of offices in six US cities. *Building and Environment*, *60*, 243-253.

Rackes, A., & Waring, M. S. (2015). Do time-averaged, whole-building, effective volatile organic compound (VOC) emissions depend on the air exchange rate? A statistical analysis of trends for 46 VOCs in US offices. *Indoor air*.

Rackes, A., & Waring, M. S. (2017). Alternative ventilation strategies in US offices: Comprehensive assessment and sensitivity analysis of energy saving potential. *Building and Environment*, *116*, 30-44.

Sidheswaran, M. A., Destaillats, H., Sullivan, D. P., Cohn, S., & Fisk, W. J. (2012). Energy efficient indoor VOC air cleaning with activated carbon fiber (ACF) filters. *Building and Environment*, *47*, 357-367.

Soreanu, G., Dixon, M., & Darlington, A. (2013). Botanical biofiltration of indoor gaseous pollutants–A mini-review. *Chemical engineering journal*, *229*, 585-594.

Sundell, J., Levin, H., Nazaroff, W. W., Cain, W. S., Fisk, W. J., Grimsrud, D. T., ... & Samet, J. M. (2011). Ventilation rates and health: multidisciplinary review of the scientific literature. *Indoor air*, *21*(3), 191-204.

Todd, N. J., & Todd, J. (1994). *From eco-cities to living machines: principles of ecological design*. North Atlantic Books.

U.S. Department of Energy (DOE). (2012). Energy Efficiency and Renewable Energy. 2011 Buildings Energy Data Book – 3.1: Commercial Sector Energy Consumption.

U.S. Energy Information Administration (EIA). (2017). Commercial Buildings Energy Consumption Survey (CBECS) Data – Table E1. Major Fuel Consumption (Btu) by End Use for Non-Mall Buildings, 2003, 2006 https://www.eia.gov/consumption/commercial/data/2003/index.php?view=consumption (accessed June 11, 2017).

U.S. Energy Information Administration (EIA). (2016a). Fossil fuels still dominate U.S. energy consumption despite recent market share decline. https://www.eia.gov/todayinenergy/detail.php?id=26912 (accessed June 11, 2017).

U.S. Energy Information Administration (EIA). (2016b). Average retail price of electricity to ultimate customers - Annual, by sector, by state, by provider, 1990-2014 n.d. http://www.eia.gov/electricity/data/state/avgprice_annual.xls (accessed April 27, 2016).

U.S. Energy Information Administration (EIA). (2016c). Natural Gas Prices - Average Commercial Price n.d. https://www.eia.gov/dnav/ng/ng_pri_sum_a_EPG0_PCS_DMcf_m.htm (accessed April 27, 2016).

U.S. Energy Information Administration (EIA). (2016d). Natural Gas Consumption by End Use - Natural Gas Delivered to Commercial Consumers n.d. http://www.eia.gov/dnav/ng/ng_cons_sum_a_epg0_vcs_mmcf_m.htm (accessed April 27, 2016).

U.S. Energy Information Administration (EIA). (2016e). Retail sales of electricity to ultimate customers - Annual, by sector, by state, by provider, 1990-2014 n.d. http://www.eia.gov/electricity/data/state/sales_annual.xls (accessed April 27, 2016).

U.S. Environmental Protection Agency (EPA). (2017a). The inside story: a guide to indoor air quality. n.d. https://www.epa.gov/indoor-air-quality-iaq/inside-story-guide-indoor-air-quality (accessed June 11, 2017)

U.S. Environmental Protection Agency (EPA). (2017b). Improving indoor air quality. n.d. https://www.epa.gov/indoor-air-quality-iaq/improving-indoor-air-quality (accessed June 11, 2017)

U.S. Environmental Protection Agency (EPA). (2017c). Volatile organic compounds' impact on indoor air quality. n.d. https://www.epa.gov/indoor-air-quality-iaq/volatile-organic-compounds-impact-indoor-air-quality (accessed June 11, 2017)

Cowan, S., & Van Der Ryn, S. (1996). Ecological design. *Washington: DC-Covelo*.

Wallace, L. A. (2001). Human exposure to volatile organic pollutants: implications for indoor air studies 1. *Annual Review of Energy and the Environment*, *26*(1), 269-301.

Wargocki, P., Sundell, J., Bischof, W., Brundrett, G., Fanger, P. O., Gyntelberg, F., ... & Wouters, P. (2002). Ventilation and health in non-industrial indoor environments: report from a European Multidisciplinary Scientific Consensus Meeting (EUROVEN). *Indoor air*, *12*(2), 113-128.

Waring, M. S. (2014). Secondary organic aerosol in residences: predicting its fraction of fine particle mass and determinants of formation strength. *Indoor Air*, *24*(4), 376-389.

Wieslander, G., Norbäck, D., & Edling, C. (1997). Airway symptoms among house painters in relation to exposure to volatile organic compounds (VOCS)—a longitudinal study. *The Annals of occupational hygiene*, *41*(2), 155-166.

Wolverton, B. C., Johnson, A., & Bounds, K. (1989). Interior landscape plants for indoor air pollution abatement.

World Commission on Environment and Development. (1987) *Our Common Future*. N.p.: Oxford, U.

Yu, C., & Crump, D. (1998). A review of the emission of VOCs from polymeric materials used in buildings. *Building and Environment, 33*(6), 357-374.